Electronic Supplementary Information (ESI) for: Narrowing the Gap Between Experimental and Computational Determination of Methyl Group Dynamics in Proteins

Falk Hoffmann,[†] Mengjun Xue,[‡] Lars V. Schäfer,[*,†] and Frans A. A. Mulder[*,‡]

[†]*Theoretical Chemistry, Ruhr-University Bochum, D-44780 Bochum, Germany*

[‡]*Interdisciplinary Nanoscience Center (iNANO) and Department of Chemistry, University of Aarhus, DK-8000 Aarhus, Denmark*

E-mail: lars.schaefer@ruhr-uni-bochum.de; fmulder@chem.au.dk

Phone: +49 234 3221582; +45 87155889

Table S1: Methyl order parameter from NMR relaxation using the isotropic model with $\tau_R = 10.70\,\text{ns}$. Values in red and bold are methyl groups that could likely be subject to strong coupling.

methyl	S^2_{axis}
MET1-C^{ϵ}	0.292
ILE3-$C^{\gamma,2}$	0.654
ILE3-$C^{\delta,1}$	0.484
MET6-C^{ϵ}	0.971
LEU7-$C^{\delta,1}$	0.403
LEU7-$C^{\delta,2}$	0.378
ILE9-$C^{\gamma,2}$	0.786
ILE9-$C^{\delta,1}$	0.746
LEU13-$C^{\delta,1}$	0.428
LEU13-$C^{\delta,2}$	0.424
LEU15-$C^{\delta,1}$	0.686
LEU15-$C^{\delta,2}$	0.728
ILE17-$C^{\gamma,2}$	0.588
ILE17-$C^{\delta,1}$	0.746
THR21-C^{γ}	0.282
ILE27-$C^{\gamma,2}$	0.792
ILE27-$C^{\delta,1}$	0.444
ILE29-$C^{\gamma,2}$	0.865
ILE29-$C^{\delta,1}$	0.493
LEU32-$C^{\delta,1}$	0.275
LEU32-$C^{\delta,2}$	0.308
LEU33-$C^{\delta,1}$	**0.894**
LEU33-$C^{\delta,2}$	0.729
LEU39-$C^{\delta,1}$	0.632
LEU39-$C^{\delta,2}$	0.543
ALA41-C^{β}	0.783
ALA42-C^{β}	0.810
LEU46-$C^{\delta,1}$	0.520
LEU46-$C^{\delta,2}$	**0.747**
ALA49-C^{β}	0.855
ILE50-$C^{\gamma,2}$	0.621

methyl	S^2_{axis}
ILE50-$C^{\delta,1}$	0.600
VAL57-$C^{\gamma,1}$	0.410
VAL57-$C^{\gamma,2}$	0.412
ILE58-$C^{\gamma,2}$	0.790
ILE58-$C^{\delta,1}$	0.816
ALA63-C^{β}	0.899
LEU66-$C^{\delta,1}$	0.460
LEU66-$C^{\delta,2}$	0.435
VAL71-$C^{\gamma,1}$	0.549
VAL71-$C^{\gamma,2}$	0.701
ALA73-C^{β}	0.921
ALA74-C^{β}	0.844
VAL75-$C^{\gamma,1}$	0.754
VAL75-$C^{\gamma,2}$	0.712
ILE78-$C^{\gamma,2}$	0.900
ILE78-$C^{\delta,1}$	0.704
LEU79-$C^{\delta,1}$	**0.854**
LEU79-$C^{\delta,2}$	0.620
ALA82-C^{β}	0.753
LEU84-$C^{\delta,1}$	**0.661**
LEU84-$C^{\delta,2}$	0.655
VAL87-$C^{\gamma,1}$	0.556
VAL87-$C^{\gamma,2}$	0.571
LEU91-$C^{\delta,1}$	**0.766**
LEU91-$C^{\delta,2}$	0.798
ALA93-C^{β}	0.830
VAL94-$C^{\gamma,1}$	0.668
VAL94-$C^{\gamma,2}$	0.744
ALA97-C^{β}	0.794
ALA98-C^{β}	0.940

methyl	S^2_{axis}
LEU99-$C^{\delta,1}$	0.806
LEU99-$C^{\delta,2}$	**0.530**
ILE100-$C^{\gamma,2}$	0.971
ILE100-$C^{\delta,1}$	0.626
MET102-C^{ϵ}	0.695
VAL103-$C^{\gamma,1}$	0.696
VAL103-$C^{\gamma,2}$	0.937
MET106-C^{ϵ}	0.367
VAL111-$C^{\gamma,1}$	0.707
VAL111-$C^{\gamma,2}$	0.654
ALA112-C^{β}	0.830
LEU118-$C^{\delta,1}$	**0.428**
LEU118-$C^{\delta,2}$	0.703
MET120-C^{ϵ}	0.318
LEU121-$C^{\delta,1}$	0.787
LEU121-$C^{\delta,2}$	0.752
ALA129-C^{β}	0.802
ALA130-C^{β}	0.812
VAL131-$C^{\gamma,1}$	0.412
VAL131-$C^{\gamma,2}$	0.572
LEU133-$C^{\delta,1}$	**0.986**
LEU133-$C^{\delta,2}$	0.811
ALA134-C^{β}	0.807
ALA146-C^{β}	0.937
VAL149-$C^{\gamma,1}$	0.757
VAL149-$C^{\gamma,2}$	0.902
ILE150-$C^{\gamma,2}$	0.912
ILE150-$C^{\delta,1}$	0.703
ALA160-C^{β}	0.809
LEU164-$C^{\delta,1}$	**0.263**
LEU164-$C^{\delta,2}$	0.190

Table S2: Compilation of experimental NMR parameters for leucine methyl group dynamics in WT* T4L. The X-ray rotamer states of the side-chain dihedral angles χ_1 and χ_2 are extracted from the structure with PDB code 107L. The sign of the chemical shift difference $\Delta\delta(^{13}C^{\delta,1} - ^{13}C^{\delta,2})$ provides χ_2 from NMR following Mulder.[S1] The NMR rotamer state of χ_1 follows from the implicit assumption that χ_1/χ_2 rotamers are correlated. The ordering of large/small $^3J_{CC}$ coupling constants provides the same information.[S1] The data for $^3J_{CC}$ was taken from Mulder et al.[S2]

LEU	rotamer χ_1/χ_2 (Xray)	rotamer χ_1/χ_2 (NMR)	$\Delta\delta$ [ppm]	$^3J_{CC}$ [Hz]	LS model	S^2_{axis}	τ_R [ns]	τ_c^{eff} [ns]
7	mt	mt	0.84	2.5/1.4	2/2	0.44/0.41	9.8/ 9.7	
13	tp	tp	-1.50	1.4/3.9	2/2	0.47/0.46	9.7/ 9.7	
15	mt	mt	2.88	4.0/1.4	3/-	0.94/-		7.88/-
32	tp	tp	-1.10	1.7/3.2	3/3	0.46/0.47		6.32/6.86
33	mt	mt	3.45	-/0.9	-/2	-/0.79	-/10.0	
39	tp	tp	-2.67	0.9/4.1	2/2	0.62/0.57	11.0/10.1	
46	tp	tp	-3.83	-/4.5	2/2	0.86/-	11.3/ 9.8	
66	mt	mt	2.54	3.2/1.8	3/3	0.99/0.93		4.88/4.89
79	mt	mt	2.52	3.7/1.3	-/3	-/0.87		-/7.63
84	mt	mt	2.54	3.6/1.4	2/2	-/0.68	11.7/10.4	
91	mt	mt	4.37	-/1.1	-/2	-/0.79	-/10.8	
99	tp	tp	-2.81	0.8/4.0	3/3	0.71/-		7.81/-
118	mt	mt	4.51	-/1.1	2/2	-/0.75	10.3/10.0	
121	mt	mt	2.04	3.8/0.8	2/2	0.72/0.84	11.8/ 9.7	
133	mt	mt	3.54	-/0.7	2/2	-/0.8	9.7/10.9	

Table S3: Compilation of experimental NMR data for leucine methyl groups in chicken α-spectrin SH3. The data was taken from BMRB submission 15144.[S3] The $^{13}C^{\gamma}$ and $^{13}C^{\delta}$ chemical shifts are extracted from BMRB submission 11026 for a "bergerac" variant,[S4] which has an identical sequence with an 8 residue insert, and from Agarwal,[S5] respectively. The $^{13}C^{\delta}$ data is reported stereospecifically, in the order $^{13}C^{\delta,1}/^{13}C^{\delta,2}$. Values in red and bold in the second column are chemical shifts of methyl groups that could likely be subject to strong coupling. Values in red and bold in the last column are experimentally observed methyl order parameter S^2_{axis} with large (>0.1) systematic deviations in S^2_{axis} for LEU.

LEU	$\delta(^{13}C^{\gamma})$ [ppm]	$\delta(^{13}C^{\delta})$ [ppm]	S^2_{axis} (pyruvate)	S^2_{axis} (glucose)	ΔS^2_{axis} (glu-pyr)
8	26.3	22.4/**24.7**	0.61/0.71	0.67/**0.97**	0.06/**0.26**
10	26.5	**25.7**/23.3	0.67/0.60	0.67/0.65	0.00/0.05
12	25.9	21.1/**24.7**	0.67/0.72	0.69/**0.55**	0.02/**-0.17**
31	27.5	**26.8**/**26.5**	0.30/0.33	-/-	-/-
33	26.1	**24.7**/23.0	0.71/0.77	0.74/0.69	0.03/-0.08
34	26.3	21.4/**25.0**	0.63/0.65	0.64/**0.46**	0.01/**-0.19**
61	26.3	22.5/**24.9**	0.43/0.42	0.41/**0.52**	-0.02/**0.10**

Table S4: Relaxation rates (in s^{-1}) from NMR and MD.

Methyl	$R_{MD}(D_z)$	$R_{MD}(3D_z^2-2)$	$R_{MD}(D_y)$	$R_{NMR}(D_z)$	$R_{NMR}(3D_z^2-2)$	$R_{NMR}(D_y)$	$\Delta R_{MD}(D_z)$	$\Delta R_{MD}(3D_z^2-2)$	$\Delta R_{MD}(D_y)$	$\Delta R_{NMR}(D_z)$	$\Delta R_{NMR}(3D_z^2-2)$	$\Delta R_{NMR}(D_y)$
A112CB	31.10	20.82	151.50	16.04	11.18	139.63	1.09	0.80	1.23	0.42	0.27	2.91
A129CB	12.15	8.93	133.25	12.67	9.39	132.25	0.22	0.18	0.74	0.60	0.35	3.73
A130CB	28.69	19.49	150.16	24.52	15.93	145.95	0.51	0.52	1.25	0.93	0.59	4.72
A134CB	22.73	15.42	146.34	13.11	9.72	133.34	0.50	0.29	0.78	0.35	0.25	2.97
A146CB	97.45	93.18	287.50	41.46	34.53	183.53	1.00	1.35	8.07	6.95	4.51	19.97
A41CB	32.27	21.26	156.59	37.56	25.24	156.24	1.11	0.73	1.28	1.99	1.34	5.97
A42CB	15.71	11.24	141.23	15.57	10.92	136.08	0.54	0.35	0.84	0.48	0.24	2.47
A49CB	19.51	13.60	145.17	20.12	13.88	147.95	0.77	0.53	0.94	0.58	0.37	3.71
A63CB	17.35	12.25	139.94	22.89	16.37	158.17	1.12	0.72	1.06	1.11	0.66	6.26
A73CB	14.03	9.90	147.93	15.90	11.09	153.60	0.37	0.22	0.55	0.41	0.26	3.77
A74CB	22.39	15.24	145.50	24.62	16.76	151.44	1.41	0.91	1.45	0.81	0.61	4.55
A82CB	16.51	11.45	129.67	17.21	11.97	129.24	0.11	0.08	0.45	0.34	0.20	2.23
A93CB	16.64	11.55	131.35	21.15	14.53	145.20	0.14	0.13	0.35	0.52	0.33	3.39
A97CB	7.95	6.41	130.73	32.46	22.83	151.74	0.26	0.16	0.43	1.68	1.21	6.21
A98CB	7.42	5.93	146.62	14.54	9.77	155.22	0.26	0.17	1.08	0.80	0.48	7.48
I100CD	4.33	4.22	113.97	7.32	6.58	99.76	0.18	0.12	1.59	0.30	0.22	1.70
I100CG2	17.02	12.07	151.21	14.53	10.72	160.43	0.39	0.28	0.89	0.72	0.41	5.47
I150CD	3.78	3.87	120.53	6.51	5.83	110.52	0.03	0.02	0.50	0.39	0.28	2.58
I150CG2	10.81	7.86	145.38	11.91	8.01	147.99	0.18	0.19	0.60	0.60	0.36	4.51
I17CD	4.84	4.40	123.84	8.06	6.85	118.71	0.09	0.06	0.80	0.46	0.32	3.18
I17CG2	8.76	6.73	121.90	17.35	12.80	104.43	0.34	0.24	2.00	0.55	0.35	2.02
I27CD	9.61	8.35	80.19	12.28	8.36	77.83	0.60	0.51	5.09	0.41	0.27	1.34
I27CG2	16.40	11.51	126.90	23.12	16.25	141.88	2.35	1.59	2.69	1.17	0.81	4.76
I29CD	7.25	6.02	86.27	10.30	7.31	82.84	0.73	0.62	4.28	0.47	0.29	1.64
I29CG2	8.18	6.20	131.83	8.93	6.90	137.58	0.60	0.36	1.51	0.66	0.40	4.76
I3CD	7.87	6.26	109.23	8.13	6.39	79.28	0.42	0.42	6.71	0.24	0.16	1.10
I3CG2	6.46	5.33	121.84	11.66	9.37	108.23	0.63	0.38	1.31	0.55	0.36	2.93
I50CD	4.70	4.17	120.07	6.10	5.45	94.22	0.17	0.12	0.75	0.61	0.46	3.36
I50CG2	15.47	11.58	118.70	23.37	16.04	115.59	0.50	0.34	3.55	0.79	0.48	2.42
I58CD	18.47	12.57	149.62	15.26	11.87	136.80	0.98	0.75	1.52	0.79	0.51	4.42
I58CG2	14.59	10.29	126.05	15.66	10.68	133.08	0.57	0.34	0.81	0.73	0.42	3.96
I78CD	3.25	3.50	116.98	4.36	4.30	108.47	0.06	0.04	0.51	0.34	0.25	2.48
I78CG2	3.32	3.31	133.39	5.61	5.32	139.50	0.07	0.04	0.33	0.44	0.30	4.31
I9CD	9.04	8.51	55.74	13.24	9.44	124.08	0.45	0.47	2.53	0.64	0.46	3.66
I9CG2	10.90	8.35	111.74	19.03	12.87	136.13	0.42	0.37	3.68	0.81	0.49	4.40
L118CD2	11.43	8.40	124.09	14.66	11.39	118.75	0.30	0.19	1.44	1.08	0.75	4.41

Continued on next page

Continued from previous page

Methyl	$R_{MD}(D_z)$	$R_{MD}(3D_z^2-2)$	$R_{MD}(D_y)$	$R_{NMR}(D_z)$	$R_{NMR}(3D_z^2-2)$	$R_{NMR}(D_y)$	$\Delta R_{MD}(D_z)$	$\Delta R_{MD}(3D_z^2-2)$	$\Delta R_{MD}(D_y)$	$\Delta R_{NMR}(D_z)$	$\Delta R_{NMR}(3D_z^2-2)$	$\Delta R_{NMR}(D_y)$
L121CD1	13.01	9.44	144.32	18.16	11.52	135.66	0.18	0.16	0.64	2.15	1.35	10.65
L121CD2	37.66	25.71	155.69	29.84	18.66	142.55	0.58	0.60	1.68	1.77	1.15	6.70
L133CD2	8.11	6.31	127.87	12.25	9.67	132.73	0.18	0.13	1.33	1.15	0.76	6.71
L13CD1	9.36	7.14	99.27	17.89	11.93	81.03	0.64	0.52	4.04	0.38	0.23	1.15
L13CD2	13.56	9.46	104.08	11.63	8.22	74.01	0.61	0.50	4.34	0.34	0.18	1.02
L32CD1	10.09	7.89	54.81	12.74	9.03	53.11	0.48	0.33	3.72	0.23	0.13	0.51
L32CD2	12.47	8.35	64.68	13.84	9.63	59.06	0.37	0.22	1.90	0.21	0.15	0.56
L33CD2	13.29	9.45	121.67	31.25	22.14	141.28	0.58	0.36	0.70	2.94	1.69	8.89
L39CD1	7.83	6.07	115.91	11.82	8.48	105.33	0.14	0.08	1.44	0.33	0.22	1.66
L39CD2	13.79	9.83	117.49	19.39	13.32	99.88	0.20	0.15	0.91	0.45	0.31	1.83
L46CD1	24.47	16.48	145.71	18.56	12.53	137.97	1.23	0.77	1.57	1.12	0.64	5.87
L66CD1	10.31	8.02	107.75	15.51	13.05	83.16	0.95	0.93	6.53	0.81	0.56	2.40
L66CD2	13.78	12.26	83.90	14.17	12.02	78.10	2.21	1.80	4.36	0.42	0.30	1.48
L79CD2	11.02	7.83	124.81	14.24	10.73	105.93	0.20	0.12	1.61	0.57	0.38	2.80
L7CD1	44.69	34.74	125.85	30.21	20.06	90.42	4.65	3.15	14.24	1.10	0.78	2.22
L7CD2	20.81	15.33	89.57	27.97	18.49	84.20	0.84	0.65	8.74	0.89	0.61	1.77
L84CD2	12.23	9.25	118.18	20.25	13.65	117.82	0.22	0.17	1.48	1.07	0.67	4.66
L91CD2	3.01	3.26	121.86	5.36	4.42	123.62	0.46	0.35	0.76	0.54	0.29	4.14
L99CD1	17.13	11.78	108.40	17.55	12.30	94.49	0.27	0.14	1.81	0.65	0.44	2.35
M102CE	3.09	3.27	106.41	4.40	4.53	107.14	0.03	0.03	1.04	0.26	0.20	1.78
M106CE	3.39	2.93	56.72	5.05	5.44	58.89	0.11	0.08	2.67	0.14	0.10	0.56
M120CE	3.34	3.27	72.54	4.11	4.23	50.74	0.08	0.07	1.22	0.07	0.05	0.25
M6CE	3.49	3.38	116.24	3.22	3.69	148.08	0.11	0.13	2.05	0.31	0.21	3.54
V103CG1	25.34	17.94	142.47	27.37	17.86	143.90	1.41	0.96	1.78	0.83	0.56	3.65
V103CG2	5.40	4.61	138.70	17.73	12.01	158.00	0.14	0.09	0.95	0.96	0.60	7.18
V111CG1	8.23	6.61	115.34	15.52	11.81	120.21	0.76	0.63	5.33	0.66	0.48	3.15
V111CG2	20.80	15.69	128.55	23.46	15.60	120.76	1.17	0.82	5.45	1.17	0.74	4.05
V131CG1	10.60	9.10	62.56	18.76	14.40	79.15	0.54	0.46	3.78	0.13	0.09	0.41
V149CG1	15.00	10.65	134.28	12.74	9.55	125.08	0.14	0.09	0.88	0.54	0.39	3.21
V149CG2	3.86	3.63	137.04	13.24	9.32	148.02	0.08	0.05	0.33	1.06	0.55	6.42
V71CG1	12.43	9.06	99.62	19.81	13.87	100.82	0.90	0.76	7.25	0.52	0.36	2.07
V71CG2	8.96	7.46	84.05	22.71	15.15	127.25	0.84	0.71	7.17	0.59	0.37	2.81
V75CG1	21.94	15.98	112.03	27.68	18.83	139.95	2.13	1.34	4.29	0.88	0.58	3.54
V75CG2	6.27	5.89	98.38	12.31	9.38	117.54	0.28	0.29	3.12	0.43	0.27	2.55
V87CG1	4.95	4.65	110.64	13.88	10.83	95.92	0.11	0.12	1.06	0.32	0.22	1.44
V94CG1	4.75	4.36	121.31	10.53	7.69	109.69	0.07	0.04	0.33	0.52	0.29	2.98

Continued on next page

Continued from previous page

Methyl	$R_{MD}(D_z)$	$R_{MD}(3D_z^2-2)$	$R_{MD}(D_y)$	$R_{NMR}(D_z)$	$R_{NMR}(3D_z^2-2)$	$R_{NMR}(D_y)$	$\Delta R_{MD}(D_z)$	$\Delta R_{MD}(3D_z^2-2)$	$\Delta R_{MD}(D_y)$	$\Delta R_{NMR}(D_z)$	$\Delta R_{NMR}(3D_z^2-2)$	$\Delta R_{NMR}(D_y)$
V94CG2	7.66	6.14	121.52	9.20	7.01	119.50	0.10	0.06	0.39	0.34	0.21	2.44

Concluded

Figure S1: Spectral densities. The Fourier transformation of $C(t)$ from MD is shown in red and its values at 0, ω_D and $2\omega_D$ as red triangles. The LS2 and LS3 fits to these three data points are shown as dashed cyan and dashed magenta lines, respectively, and S^2_{axis}, τ_f, and (for the LS3 model) $\tau_c^{eff} (= \tau_R^{eff})$ are reported. The spectral density from NMR is shown in black. For $\tau_R^{(eff)} \geq 9\,\text{ns}$ in NMR, the LS2 model was chosen by AIC, otherwise the LS3 model.

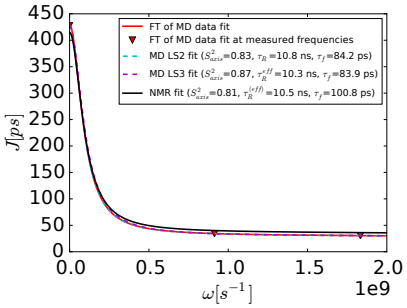

ALA41-$C^\beta H^\beta$

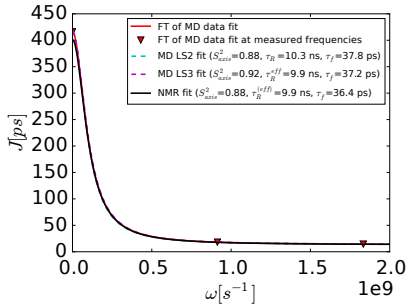

ALA42-$C^\beta H^\beta$

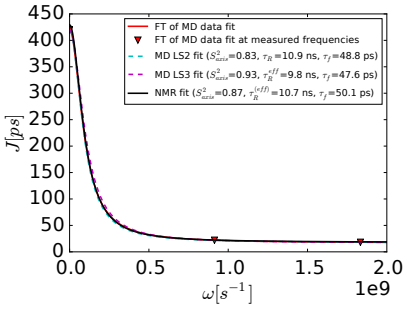

ALA49-$C^\beta H^\beta$

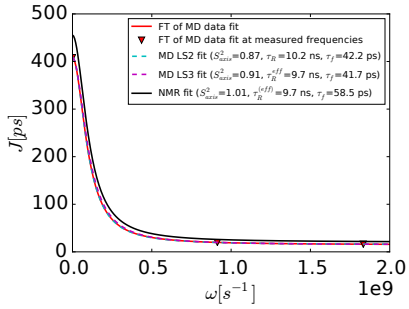

ALA63-$C^\beta H^\beta$

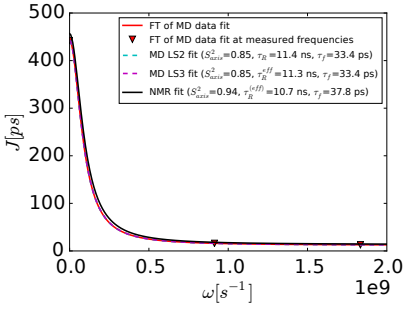

ALA73-$C^\beta H^\beta$

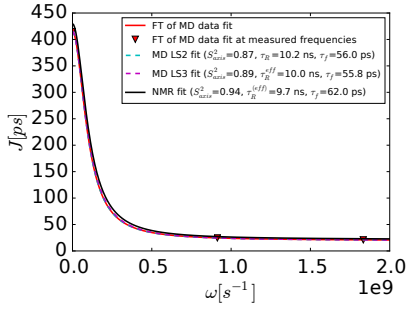

ALA74-$C^\beta H^\beta$

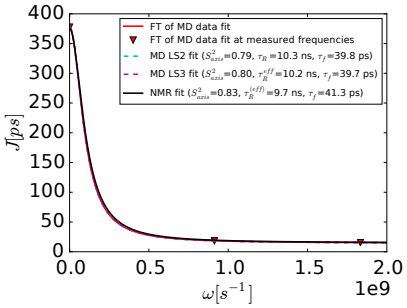

ALA82-$C^\beta H^\beta$

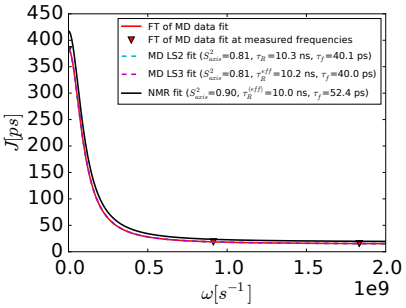

ALA93-$C^\beta H^\beta$

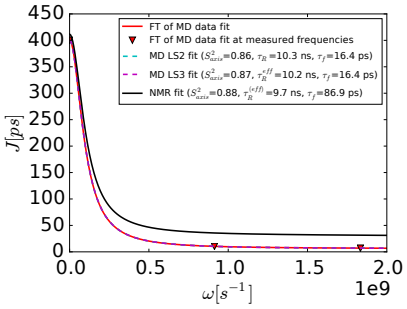

ALA97-$C^\beta H^\beta$

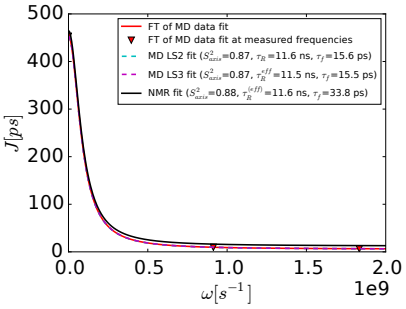

ALA98-$C^\beta H^\beta$

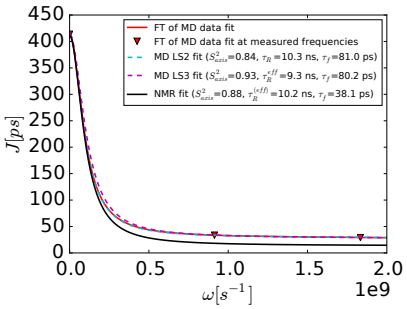

ALA112-$C^\beta H^\beta$

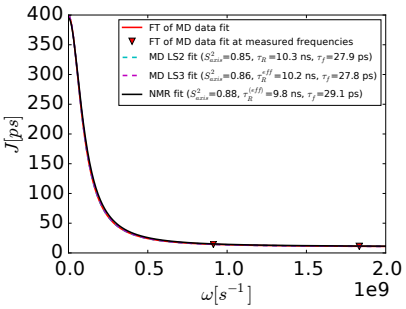

ALA129-$C^\beta H^\beta$

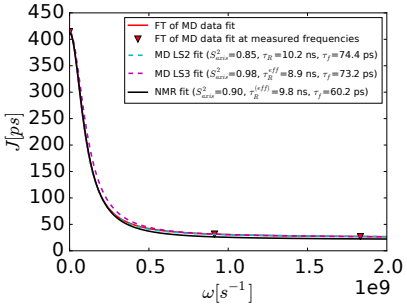

ALA130-$C^\beta H^\beta$

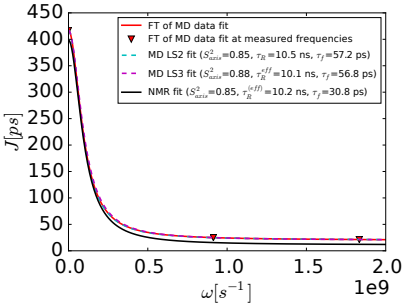

ALA134-$C^\beta H^\beta$

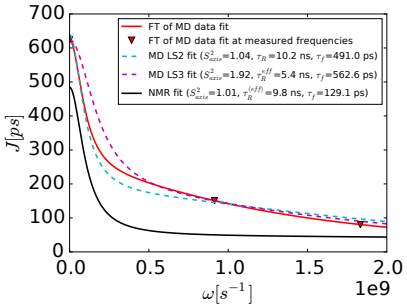

ALA146-$C^\beta H^\beta$

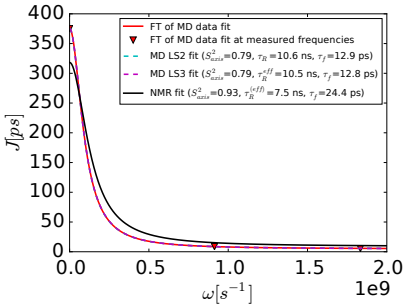

ILE3-$C^{\gamma 2}H^{\gamma 2}$

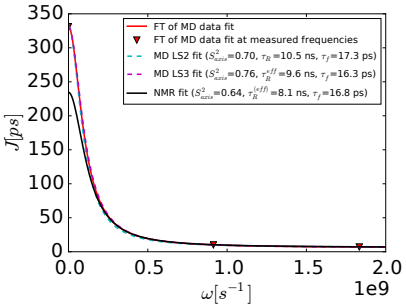

ILE3-$C^{\delta}H^{\delta}$

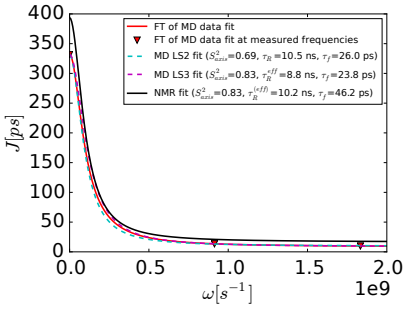

ILE9-$C^{\gamma 2}H^{\gamma 2}$

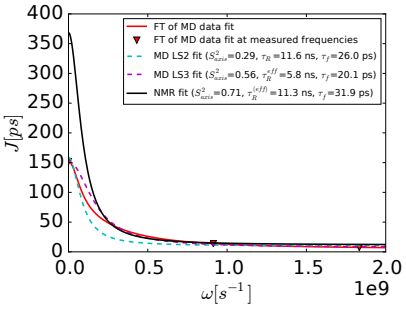

ILE9-$C^{\delta}H^{\delta}$

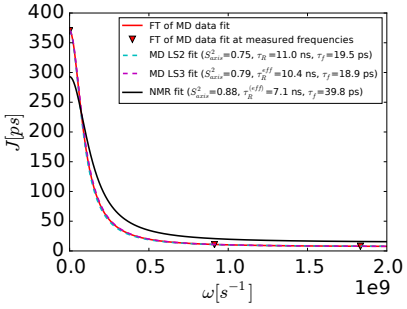

ILE17-$C^{\gamma 2}H^{\gamma 2}$

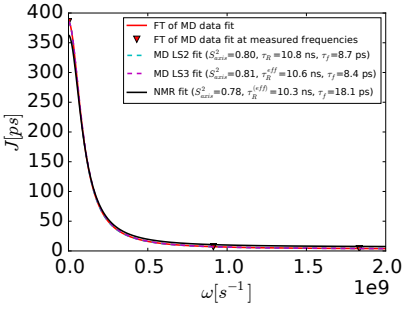

ILE17-$C^{\delta}H^{\delta}$

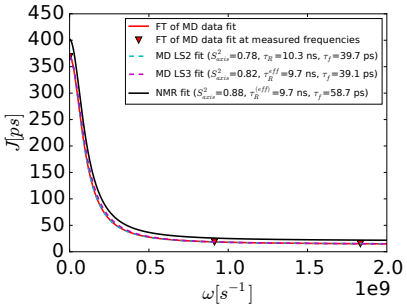

ILE27-$C^{\gamma 2}H^{\gamma 2}$

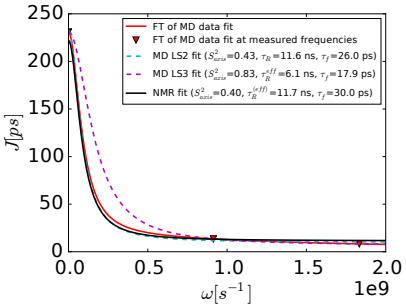

ILE27-$C^{\delta}H^{\delta}$

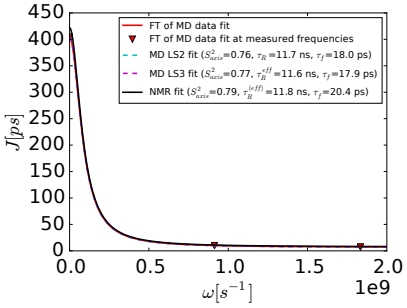

ILE29-$C^{\gamma 2}H^{\gamma 2}$

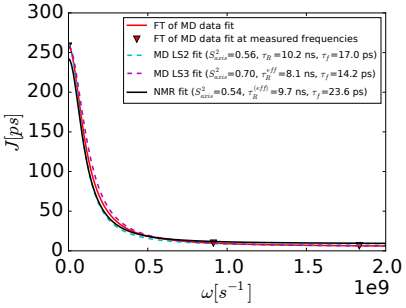

ILE29-$C^{\delta}H^{\delta}$

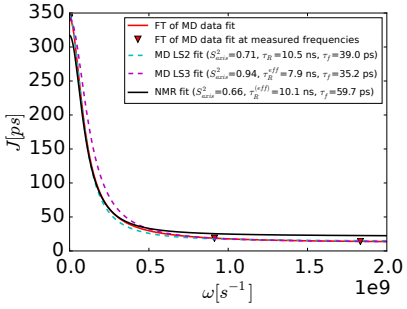

ILE50-$C^{\gamma 2}H^{\gamma 2}$

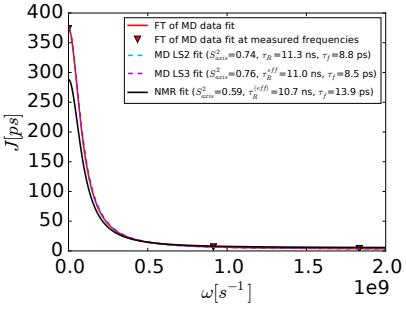

ILE50-$C^{\delta}H^{\delta}$

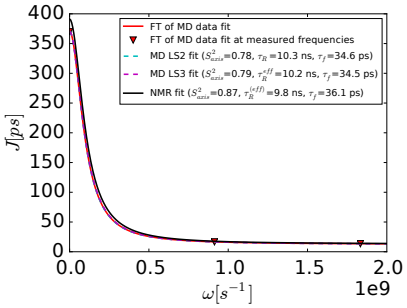

ILE58-$C^{\gamma 2}H^{\gamma 2}$

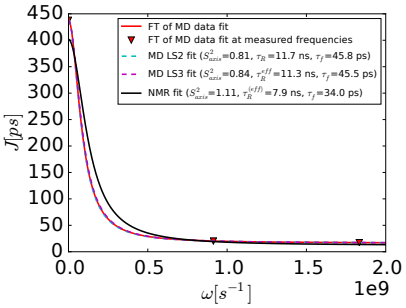

ILE58-$C^{\delta}H^{\delta}$

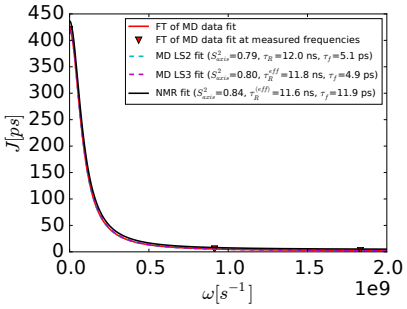

ILE78-$C^{\gamma 2}H^{\gamma 2}$

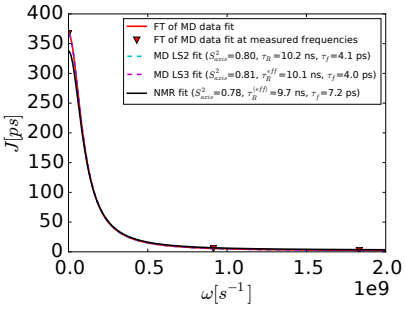

ILE78-$C^{\delta}H^{\delta}$

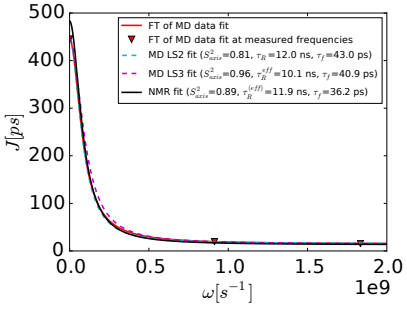

ILE100-$C^{\gamma 2}H^{\gamma 2}$

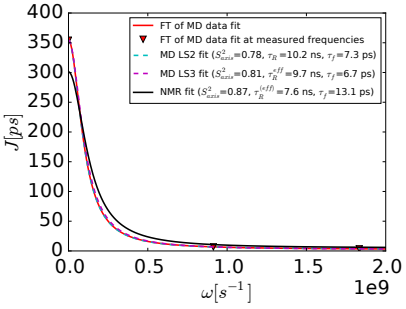

ILE100-$C^{\delta}H^{\delta}$

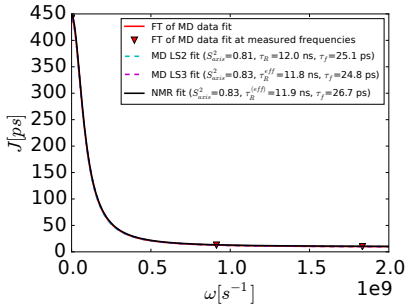

ILE150-$C^{\gamma 2}H^{\gamma 2}$

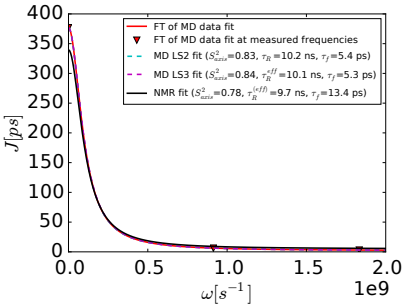

ILE150-$C^{\delta}H^{\delta}$

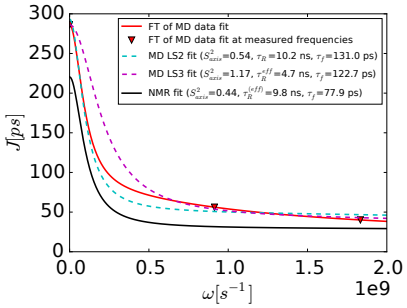

LEU7-$C^{\delta 1}H^{\delta 1}$

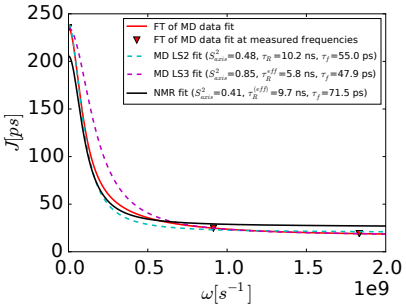

LEU7-$C^{\delta 2}H^{\delta 2}$

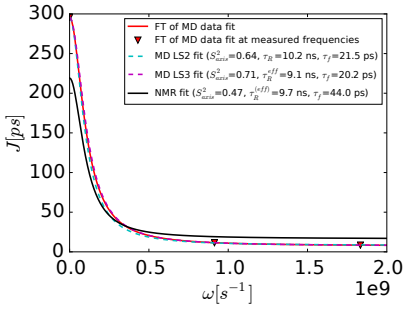

LEU13-$C^{\delta 1}H^{\delta 1}$

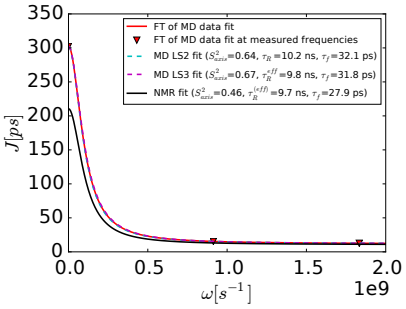

LEU13-$C^{\delta 2}H^{\delta 2}$

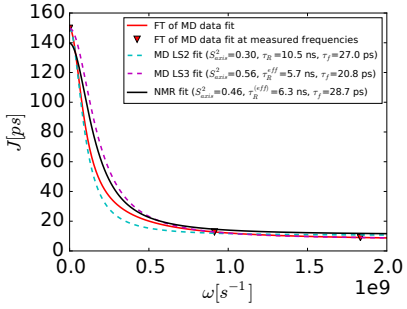

LEU32-$C^{\delta 1}H^{\delta 1}$

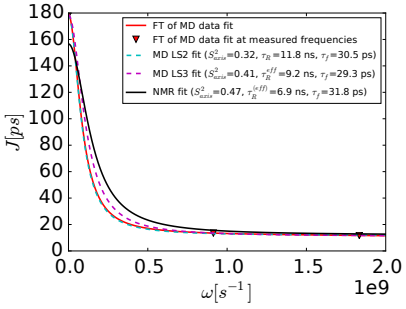

LEU32-$C^{\delta 2}H^{\delta 2}$

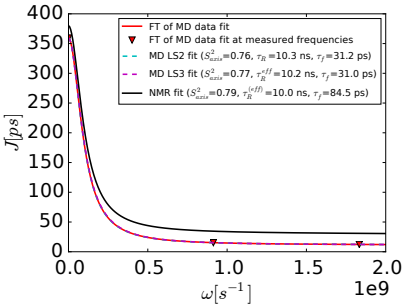

LEU33-$C^{\delta 2}H^{\delta 2}$

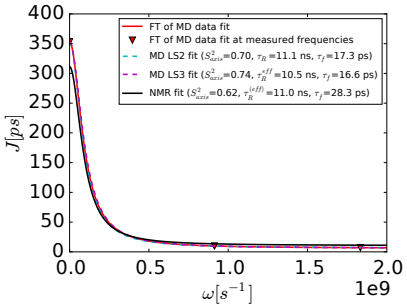

LEU39-$C^{\delta 1}H^{\delta 1}$

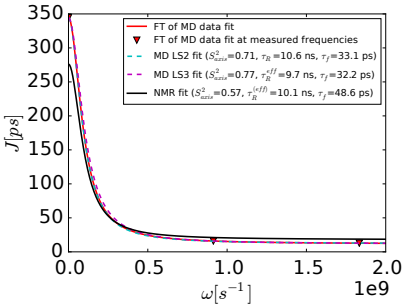

LEU39-$C^{\delta 2}H^{\delta 2}$

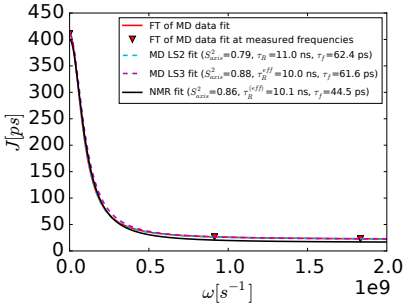

LEU46-$C^{\delta 1}H^{\delta 1}$

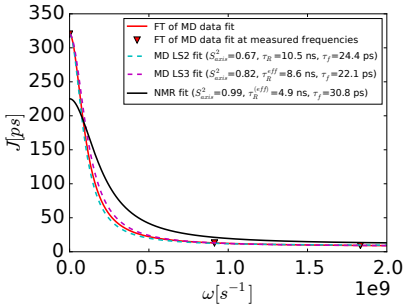

LEU66-$C^{\delta 1}H^{\delta 1}$

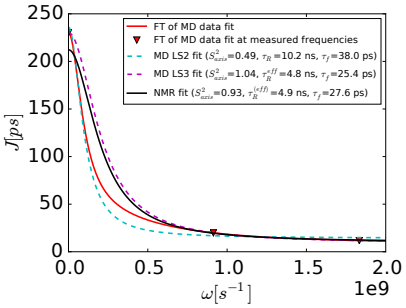

LEU66-$C^{\delta 2}H^{\delta 2}$

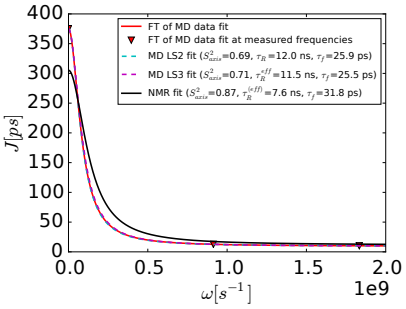

LEU79-$C^{\delta 2}H^{\delta 2}$

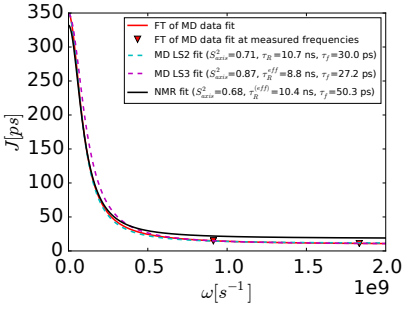

LEU84-$C^{\delta 2}H^{\delta 2}$

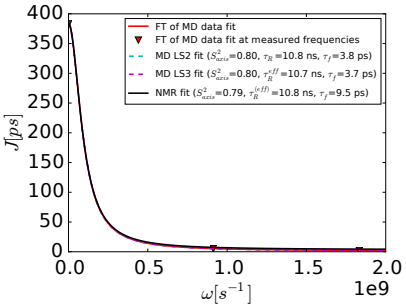

LEU91-$C^{\delta 2}H^{\delta 2}$

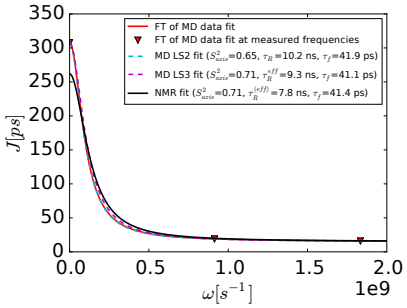

LEU99-$C^{\delta 1}H^{\delta 1}$

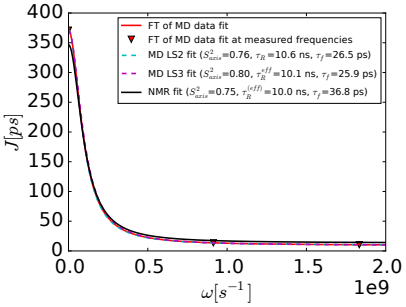

LEU118-$C^{\delta 2}H^{\delta 2}$

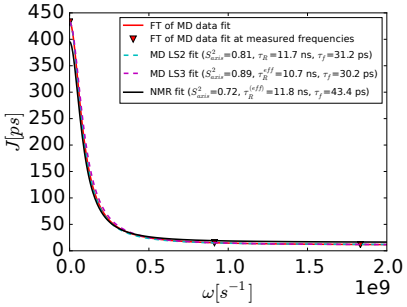

LEU121-$C^{\delta 1}H^{\delta 1}$

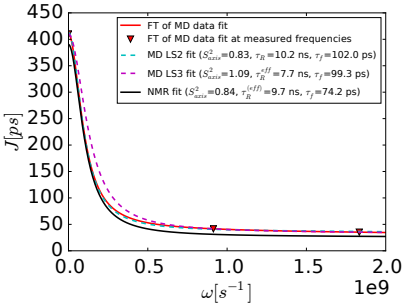

LEU121-$C^{\delta 2}H^{\delta 2}$

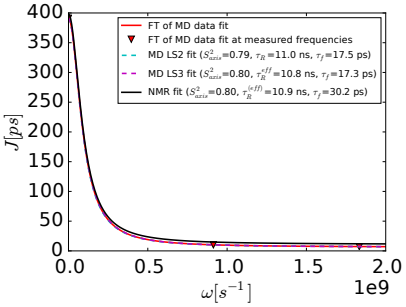

LEU133-$C^{\delta 2}H^{\delta 2}$

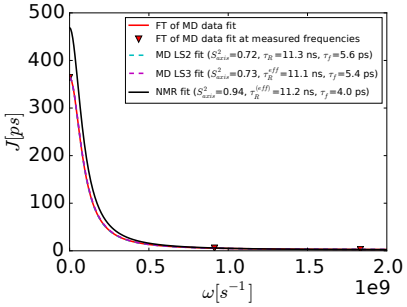

MET6-$C^{\epsilon}H^{\epsilon}$

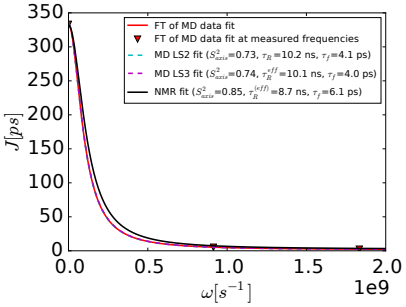

MET102-$C^{\epsilon}H^{\epsilon}$

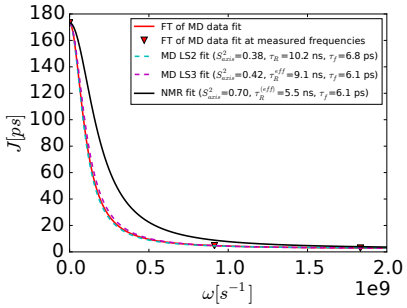

MET106-$C^{\epsilon}H^{\epsilon}$

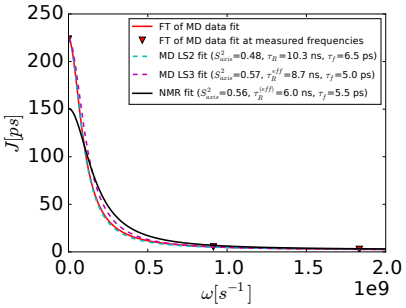

MET120-$C^{\epsilon}H^{\epsilon}$

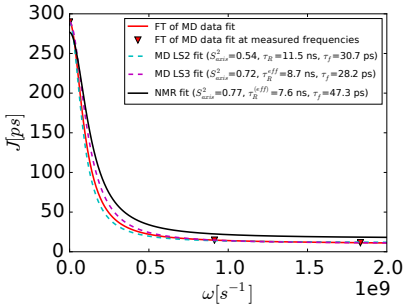

VAL71-$C^{\gamma 1}H^{\gamma 1}$

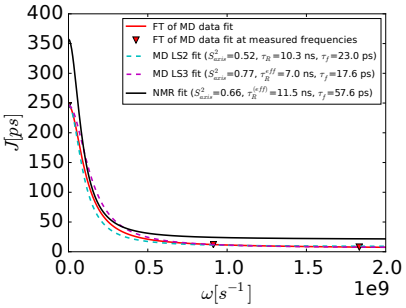

VAL71-$C^{\gamma 2}H^{\gamma 2}$

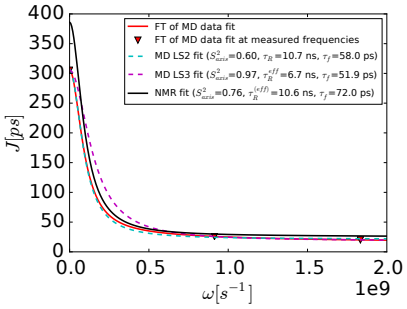

VAL75-$C^{\gamma 1}H^{\gamma 1}$

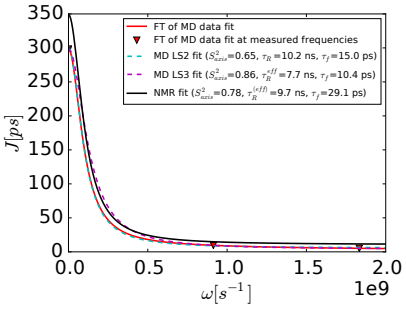

VAL75-$C^{\gamma 2}H^{\gamma 2}$

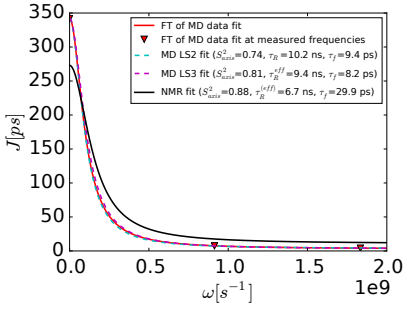

VAL87-$C^{\gamma 1}H^{\gamma 1}$

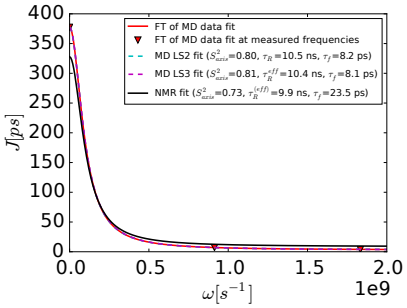

VAL94-$C^{\gamma 1}H^{\gamma 1}$

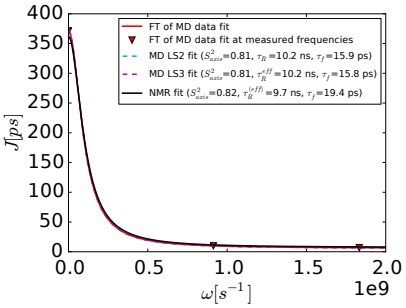

VAL94-$C^{\gamma 2}H^{\gamma 2}$

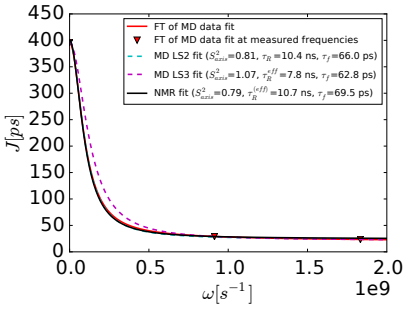

VAL103-$C^{\gamma 1}H^{\gamma 1}$

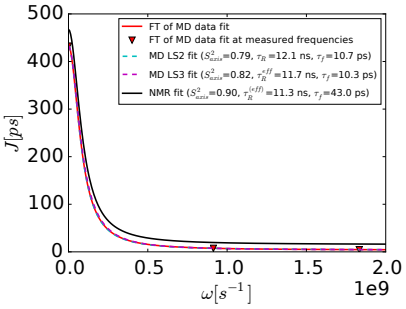

VAL103-$C^{\gamma 2}H^{\gamma 2}$

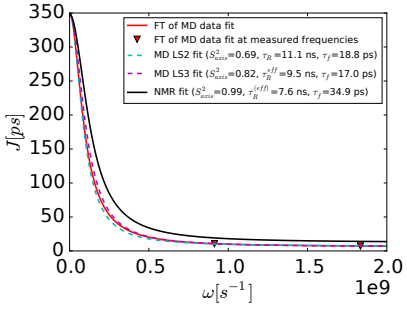

VAL111-$C^{\gamma 1}H^{\gamma 1}$

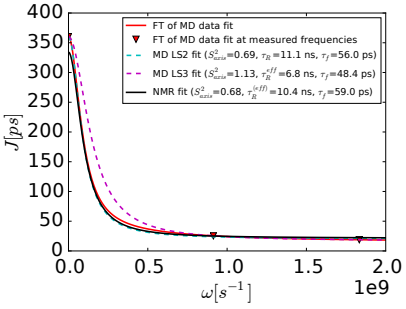

VAL111-$C^{\gamma 2}H^{\gamma 2}$

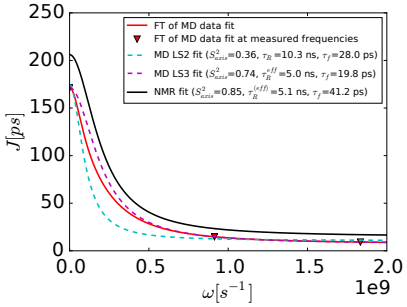

VAL131-$C^{\gamma 1}H^{\gamma 1}$

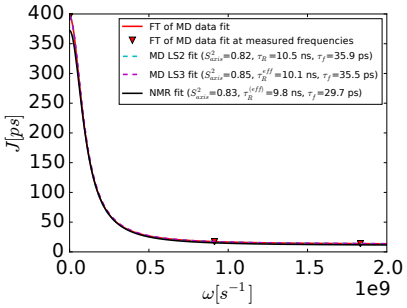

VAL149-$C^{\gamma 1}H^{\gamma 1}$

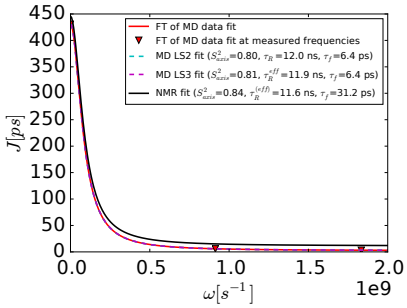

VAL149-$C^{\gamma 2}H^{\gamma 2}$

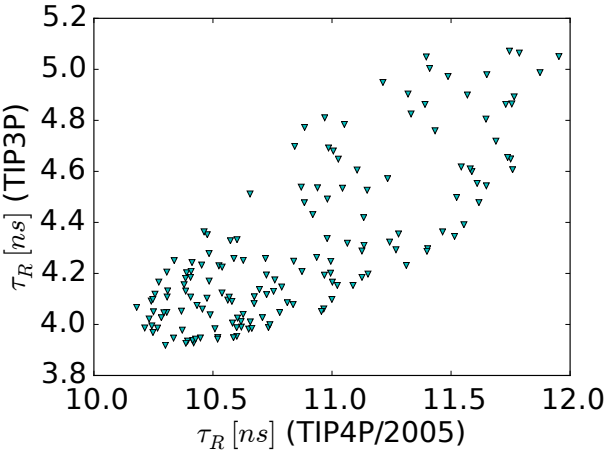

Figure S2: Rotational tumbling times of individual backbone N–H vectors, obtained with the Lipari-Szabo TCF fitting method, from the MD simulations with the TIP3P and TIP4P/2005 water models. The Pearson and Spearman correlation coefficients between the TIP3P and TIP4P/2005 data are $R_P = 0.81$ and $R_S = 0.77$, respectively.

Table S5: N-H order parameter from NMR relaxation experiments and MD simulations (TIP4P/2005 water model). Order parameters that were not determined are marked with an "x".

Residue	S^2_{NH} **(MD)**	S^2_{NH} **(NMR)**
M1	x	x
N2	0.72	0.66
I3	0.88	0.85
F4	0.91	0.85
E5	0.81	0.87
M6	0.89	x
L7	0.92	0.92
R8	0.91	0.88
I9	0.87	0.88
D10	0.88	0.89
E11	0.87	0.87
G12	0.79	0.67
L13	0.68	0.75
R14	0.84	0.77
L15	0.83	0.77
K16	0.81	0.80
I17	0.88	0.80
Y18	0.89	0.84
K19	0.83	0.78
D20	0.75	0.80
T21	0.80	0.49
E22	0.80	x
G23	0.78	0.83
Y24	0.72	0.82
Y25	0.81	0.77
T26	0.90	0.83
I27	0.92	0.86
G28	0.91	0.83
I29	0.86	0.89
G30	0.84	0.75
H31	0.84	0.85
L32	0.87	0.83
L33	0.85	0.82
T34	0.88	x
K35	0.87	x
S36	0.83	0.82
P37	x	x
S38	0.47	0.44
L39	0.86	x
N40	0.88	0.70
A41	0.87	x
A42	0.87	0.84
K43	0.91	0.79
S44	0.89	0.79
E45	0.86	x
L46	0.89	0.86
D47	0.91	0.88
K48	0.88	0.87
A49	0.86	0.85
I50	0.88	0.86
G51	0.83	0.83
R52	0.80	0.80
N53	0.84	0.74
T54	0.78	0.78
N55	0.82	0.88
G56	0.85	x
V57	0.86	0.85
I58	0.88	x
T59	0.85	0.83
K60	0.90	0.82
D61	0.89	0.81
E62	0.87	x
A63	0.91	0.85
E64	0.90	0.87
K65	0.91	0.84
L66	0.89	x
F67	0.90	0.89
N68	0.92	x
Q69	0.87	x
D70	0.89	0.83
V71	0.90	0.85
D72	0.90	0.87
A73	0.90	0.88
A74	0.87	0.81
V75	0.90	0.84
R76	0.92	0.88
G77	0.91	x
I78	0.86	0.87
L79	0.90	0.87
R80	0.78	0.86
N81	0.75	x
A82	0.83	0.87

Residue	S^2_{NH} **(MD)**	S^2_{NH} **(NMR)**
K83	0.87	0.81
L84	0.82	0.76
K85	0.87	0.85
P86	x	x
V87	0.88	0.83
Y88	0.90	0.86
D89	0.88	0.88
S90	0.81	0.79
L91	0.81	0.82
D92	0.86	0.81
A93	0.89	0.84
V94	0.87	0.83
R95	0.92	x
R96	0.93	x
A97	0.92	0.87
A98	0.94	0.86
L99	0.93	x
I100	0.92	0.91
N101	0.95	0.91
M102	0.93	0.86
V103	0.94	x
F104	0.93	0.87
Q105	0.86	0.88
M106	0.83	0.84
G107	0.86	0.82
E108	0.88	0.83
T109	0.88	0.76
G110	0.81	0.75
F111	0.84	x
A112	0.91	0.90
G113	0.87	x
F114	0.83	0.84
T115	0.87	0.73
N116	0.87	x
S117	0.89	0.80
L118	0.93	0.89
R119	0.90	x
M120	0.92	0.86
L121	0.92	0.88
Q122	0.91	x
Q123	0.89	0.81

Residue	S^2_{NH} **(MD)**	S^2_{NH} **(NMR)**
K124	0.93	0.89
R125	0.88	0.85
W126	0.89	0.83
D127	0.89	x
E128	0.84	0.82
A129	0.89	0.87
A130	0.93	0.87
V131	0.85	0.87
N132	0.87	x
L133	0.91	0.85
A134	0.91	x
K135	0.85	0.87
S136	0.53	0.44
R137	0.87	0.86
W138	0.89	0.82
Y139	0.90	0.86
N140	0.84	0.79
Q141	0.84	0.78
T142	0.87	0.79
P143	x	x
N144	0.86	0.80
R145	0.80	0.83
A146	0.85	0.90
K147	0.93	0.87
R148	0.91	x
V149	0.91	x
I150	0.93	0.92
T151	0.91	0.86
T152	0.91	0.86
F153	0.92	0.88
R154	0.90	0.88
T155	0.89	0.88
G156	0.92	0.85
T157	0.90	0.83
W158	0.87	0.84
D159	0.85	0.86
A160	0.85	0.85
Y161	0.86	0.80
K162	0.46	0.79

Figure S3: TCFs of methyl groups. The internal TCF from MD is shown in red triangles. The internal TCF from NMR is shown as a black line and was calculated from S^2_{axis} and τ_f.

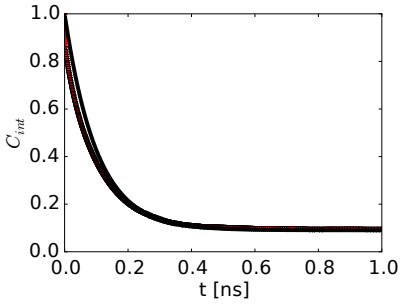

ALA41-$C^{\beta}H^{\beta}$

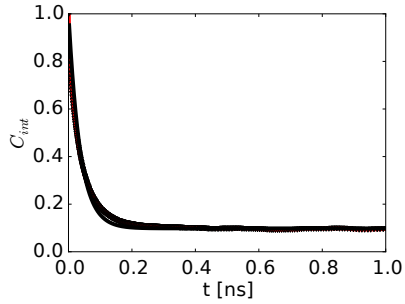

ALA42-$C^{\beta}H^{\beta}$

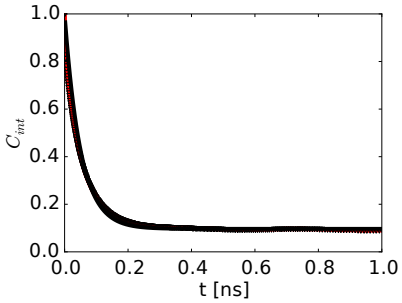

ALA49-$C^{\beta}H^{\beta}$

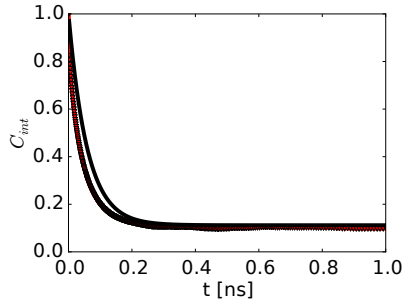

ALA63-$C^{\beta}H^{\beta}$

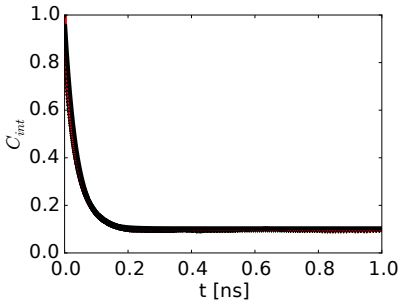

ALA73-$C^{\beta}H^{\beta}$

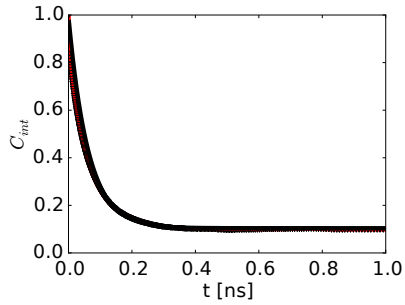

ALA74-$C^{\beta}H^{\beta}$

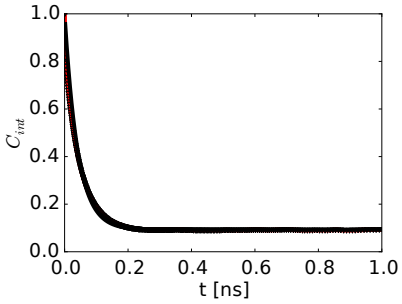

ALA82-$C^{\beta}H^{\beta}$

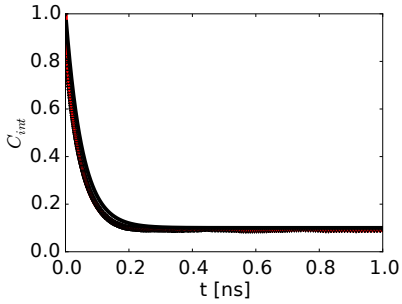

ALA93-$C^{\beta}H^{\beta}$

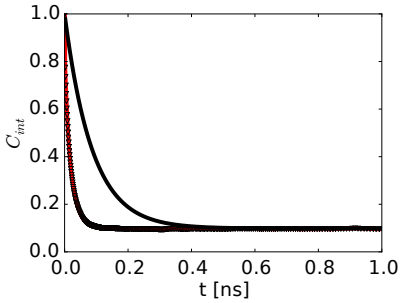

ALA97-$C^{\beta}H^{\beta}$

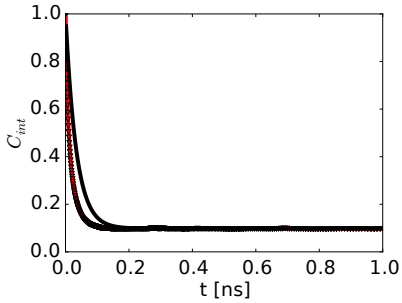

ALA98-$C^{\beta}H^{\beta}$

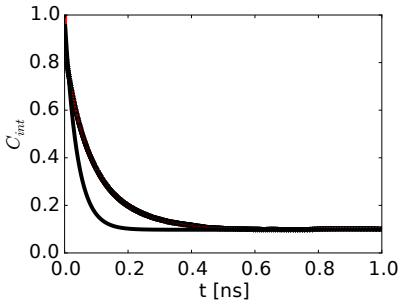

ALA112-$C^{\beta}H^{\beta}$

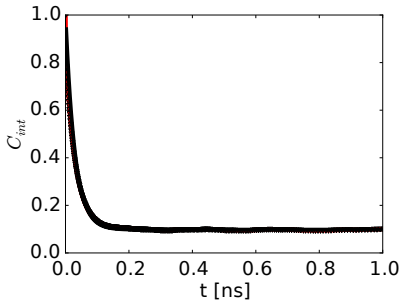

ALA129-$C^{\beta}H^{\beta}$

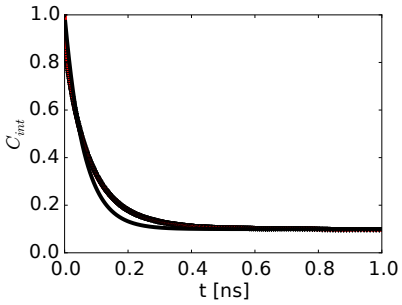

ALA130-$C^{\beta}H^{\beta}$

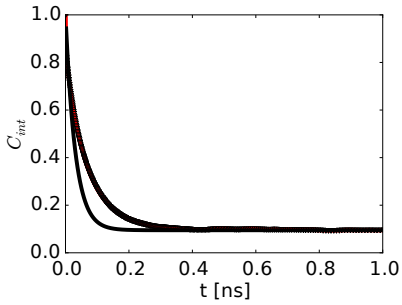

ALA134-$C^{\beta}H^{\beta}$

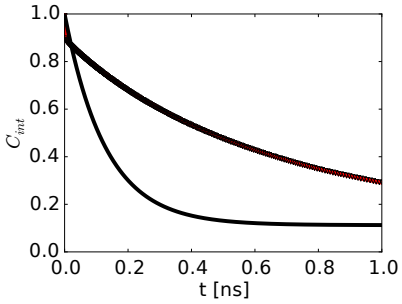

ALA146-$C^{\beta}H^{\beta}$

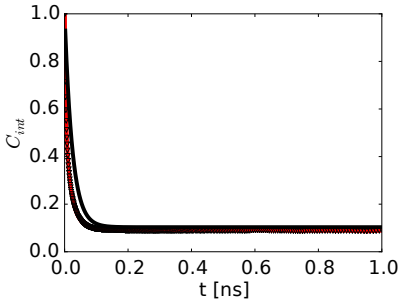

ILE3-$C^{\gamma 2}H^{\gamma 2}$

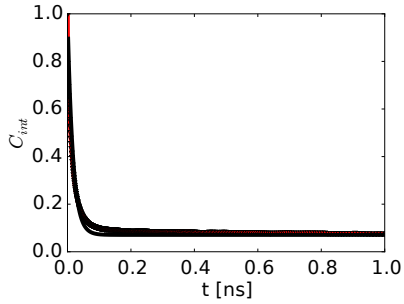

ILE3-$C^{\delta}H^{\delta}$

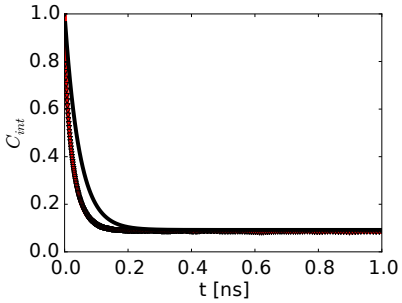

ILE9-$C^{\gamma 2}H^{\gamma 2}$

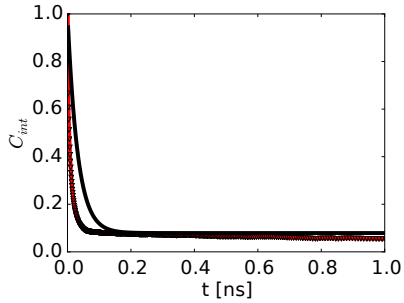

ILE9-$C^{\delta}H^{\delta}$

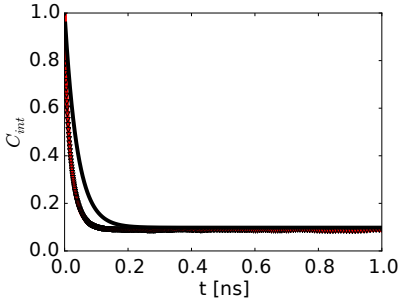

ILE17-$C^{\gamma 2}H^{\gamma 2}$

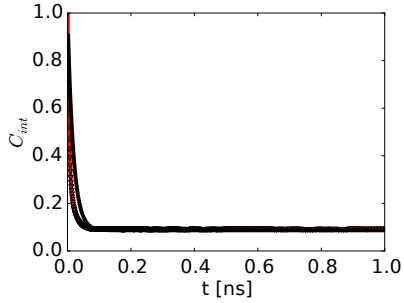

ILE17-$C^{\delta}H^{\delta}$

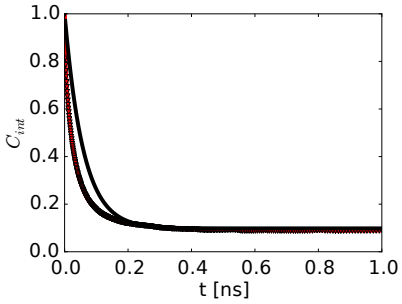

ILE27-$C^{\gamma 2}H^{\gamma 2}$

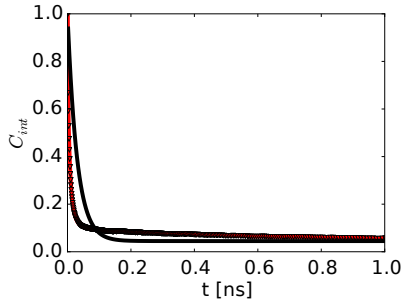

ILE27-$C^{\delta}H^{\delta}$

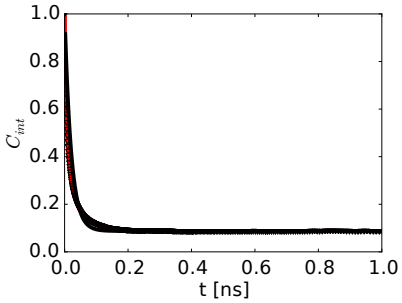

ILE29-$C^{\gamma 2}H^{\gamma 2}$

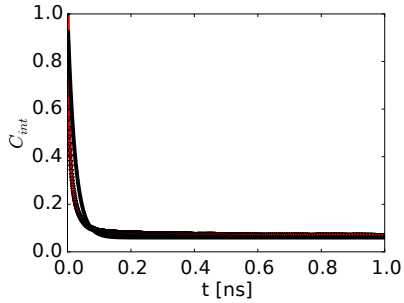

ILE29-$C^{\delta}H^{\delta}$

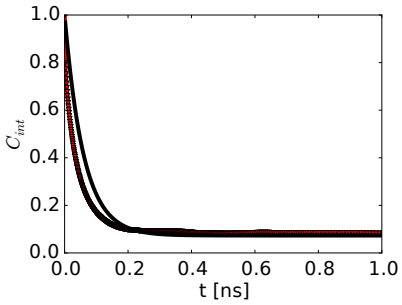

ILE50-$C^{\gamma 2}H^{\gamma 2}$

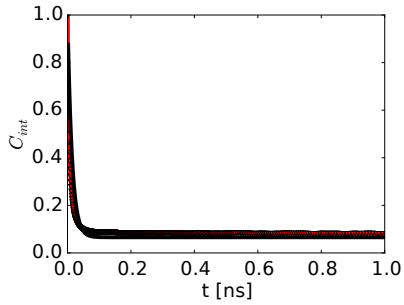

ILE50-$C^{\delta}H^{\delta}$

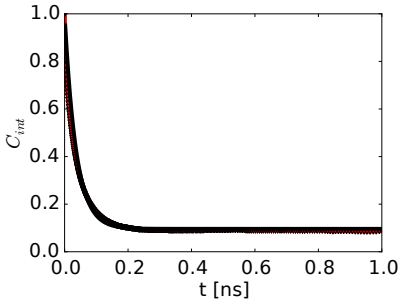

ILE58-$C^{\gamma 2}H^{\gamma 2}$

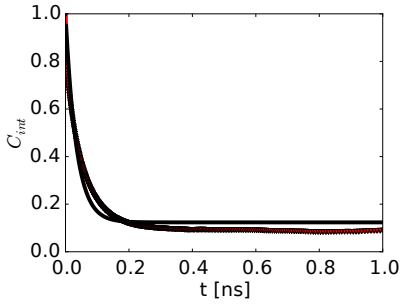

ILE58-$C^{\delta}H^{\delta}$

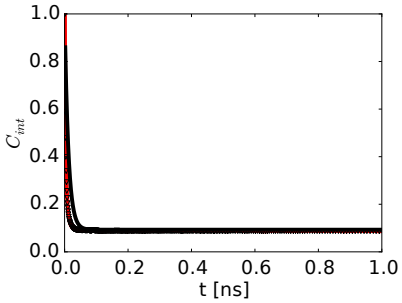

ILE78-$C^{\gamma 2}H^{\gamma 2}$

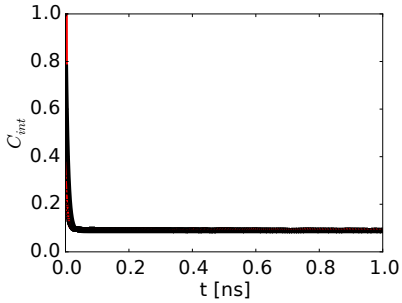

ILE78-$C^{\delta}H^{\delta}$

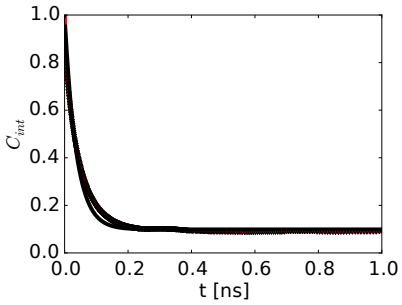

ILE100-$C^{\gamma 2}H^{\gamma 2}$

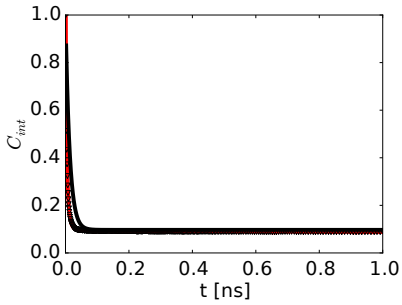

ILE100-$C^{\delta}H^{\delta}$

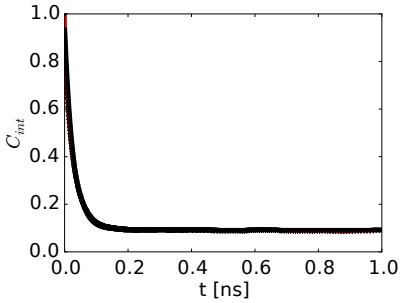

ILE150-$C^{\gamma 2}H^{\gamma 2}$

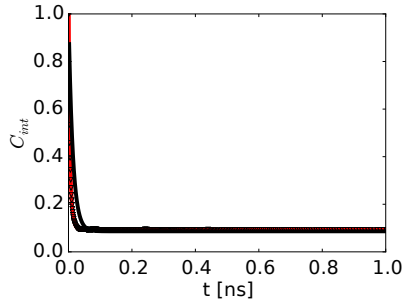

ILE150-$C^{\delta}H^{\delta}$

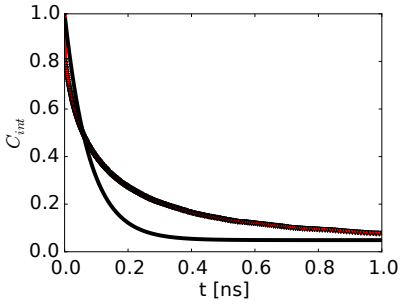

LEU7-$C^{\delta 1}H^{\delta 1}$

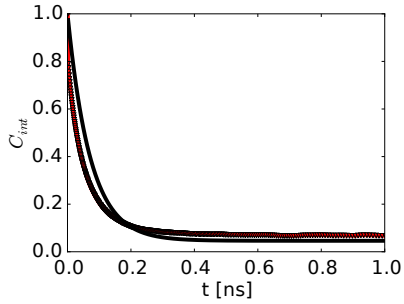

LEU7-$C^{\delta 2}H^{\delta 2}$

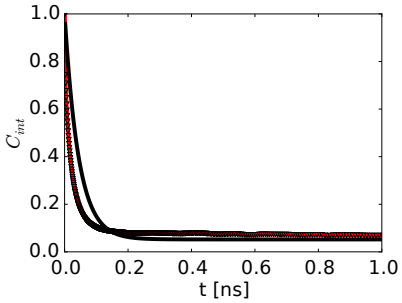

LEU13-$C^{\delta 1}H^{\delta 1}$

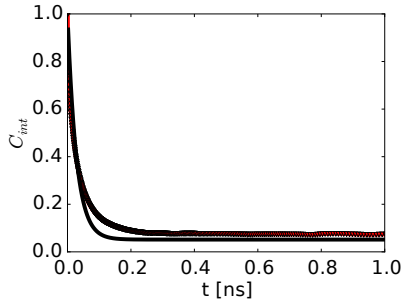

LEU13-$C^{\delta 2}H^{\delta 2}$

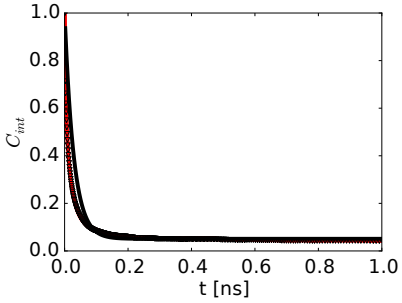

LEU32-$C^{\delta 1}H^{\delta 1}$

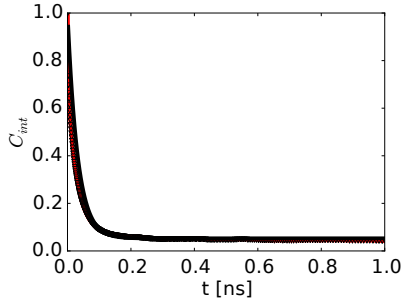

LEU32-$C^{\delta 2}H^{\delta 2}$

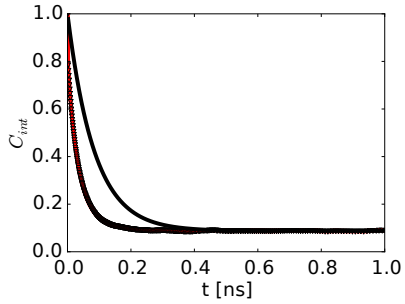

LEU33-$C^{\delta 2}H^{\delta 2}$

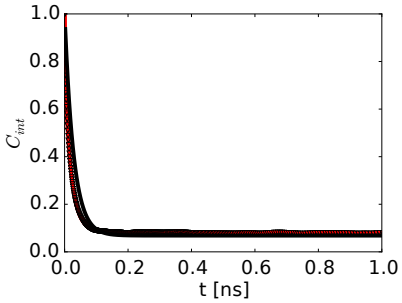

LEU39-$C^{\delta 1}H^{\delta 1}$

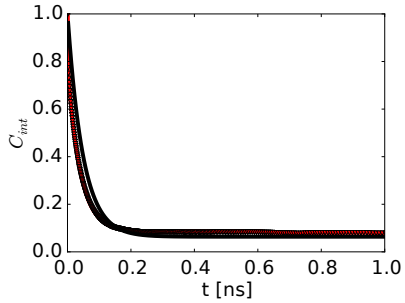

LEU39-$C^{\delta 2}H^{\delta 2}$

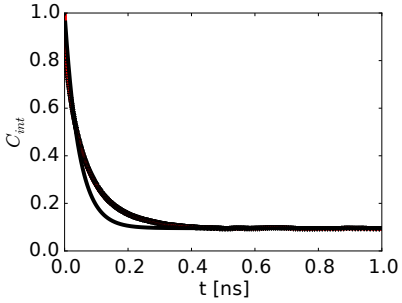

LEU46-$C^{\delta 1}H^{\delta 1}$

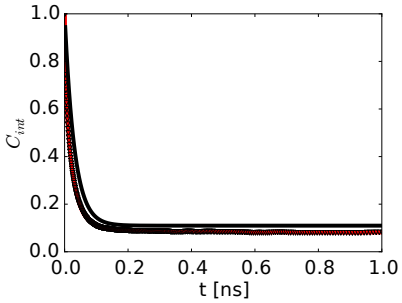

LEU66-$C^{\delta 1}H^{\delta 1}$

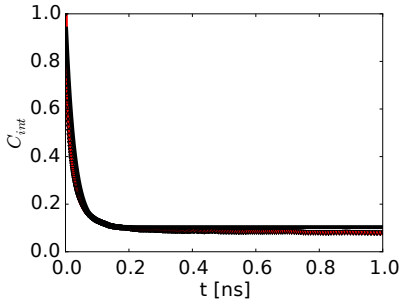

LEU66-$C^{\delta 2}H^{\delta 2}$

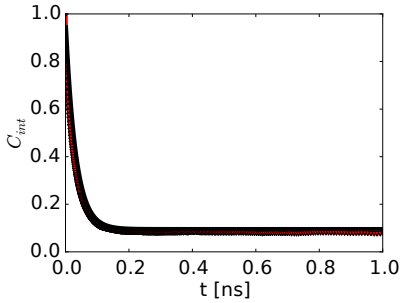

LEU79-$C^{\delta 2}H^{\delta 2}$

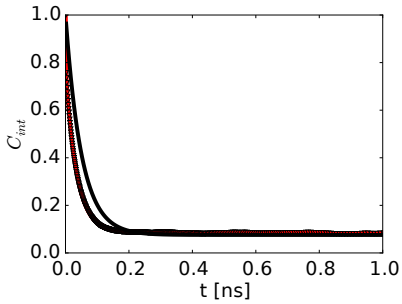

LEU84-$C^{\delta 2}H^{\delta 2}$

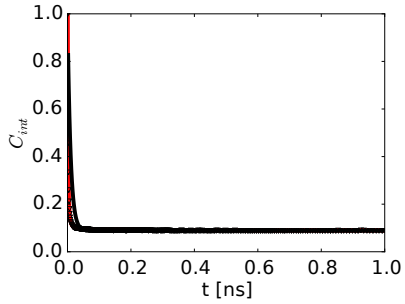

LEU91-$C^{\delta 2}H^{\delta 2}$

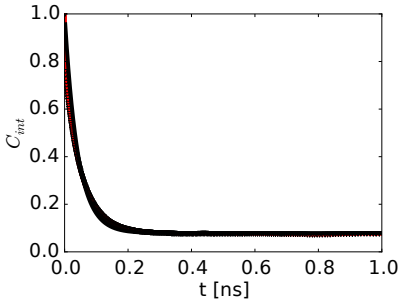

LEU99-$C^{\delta 1}H^{\delta 1}$

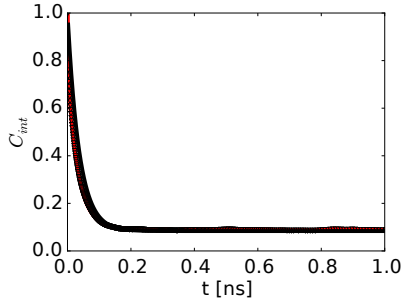

LEU118-$C^{\delta 2}H^{\delta 2}$

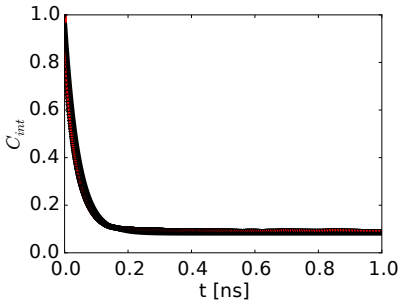

LEU121-$C^{\delta 1}H^{\delta 1}$

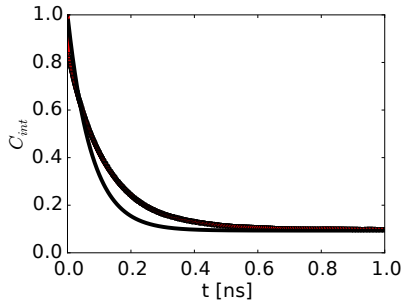

LEU121-$C^{\delta 2}H^{\delta 2}$

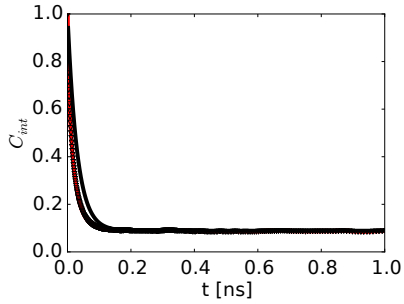

LEU133-$C^{\delta 2}H^{\delta 2}$

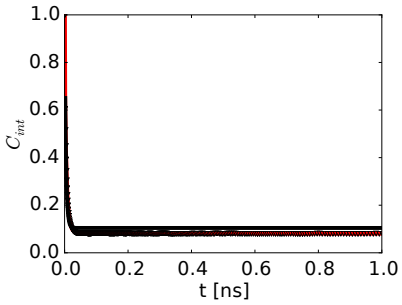

MET6-$C^{\epsilon}H^{\epsilon}$

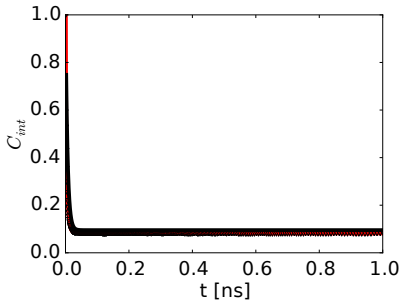

MET102-$C^{\epsilon}H^{\epsilon}$

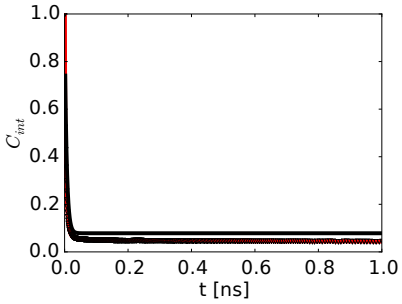

MET106-$C^{\epsilon}H^{\epsilon}$

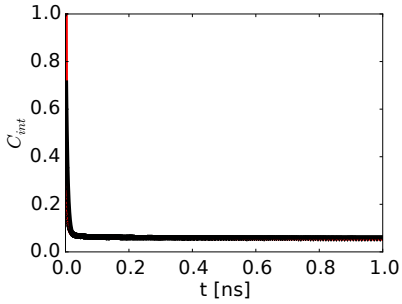

MET120-$C^{\epsilon}H^{\epsilon}$

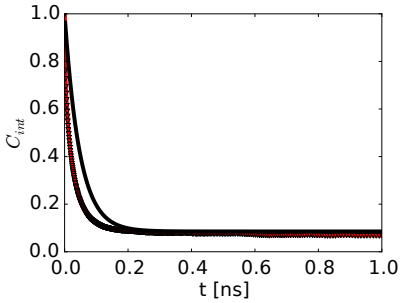

VAL71-$C^{\gamma 1}H^{\gamma 1}$

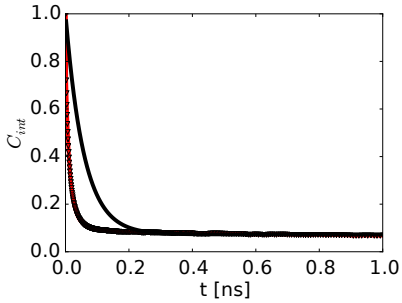

VAL71-$C^{\gamma 2}H^{\gamma 2}$

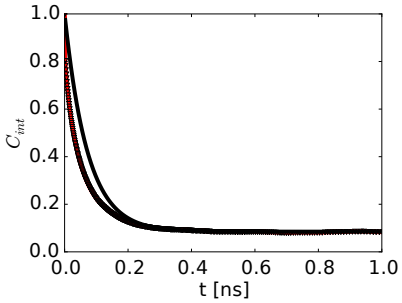

VAL75-$C^{\gamma 1}H^{\gamma 1}$

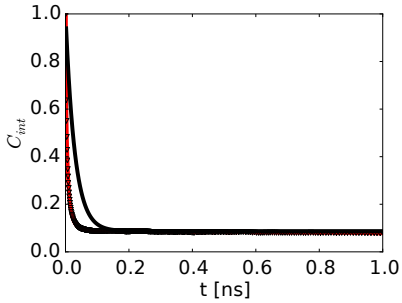

VAL75-$C^{\gamma 2}H^{\gamma 2}$

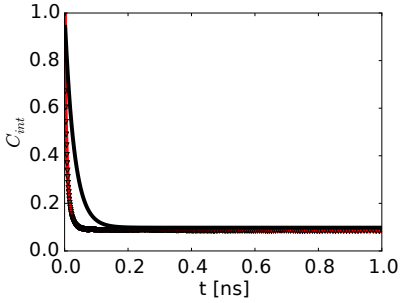

VAL87-$C^{\gamma 1}H^{\gamma 1}$

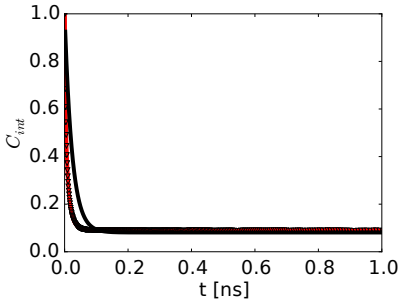

VAL94-$C^{\gamma 1}H^{\gamma 1}$

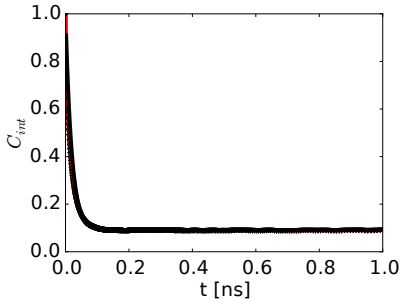

VAL94-$C^{\gamma 2}H^{\gamma 2}$

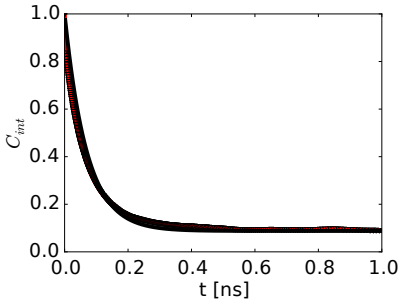

VAL103-$C^{\gamma 1}H^{\gamma 1}$

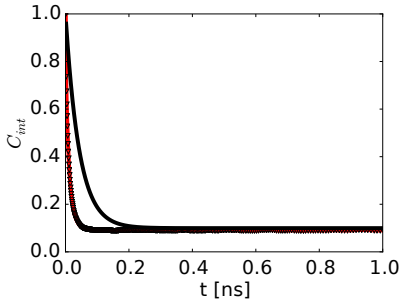

VAL103-$C^{\gamma 2}H^{\gamma 2}$

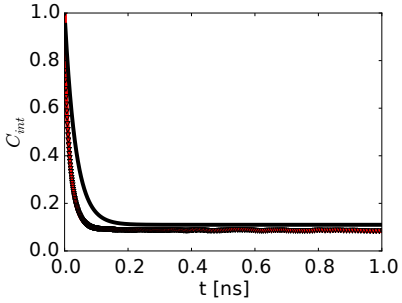

VAL111-$C^{\gamma 1}H^{\gamma 1}$

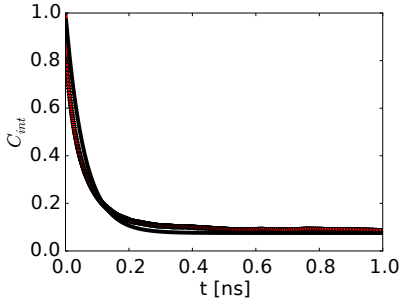

VAL111-$C^{\gamma 2}H^{\gamma 2}$

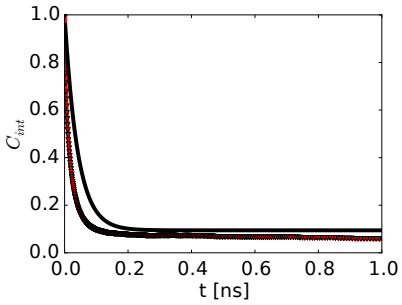

VAL131-$C^{\gamma 1}H^{\gamma 1}$

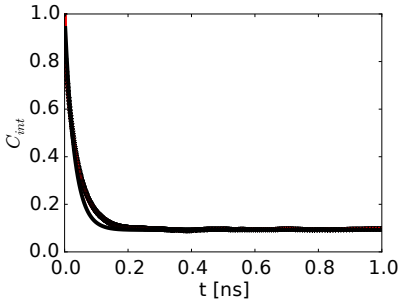

VAL149-$C^{\gamma 1}H^{\gamma 1}$

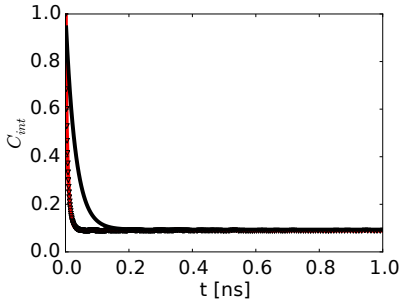

VAL149-$C^{\gamma 2}H^{\gamma 2}$

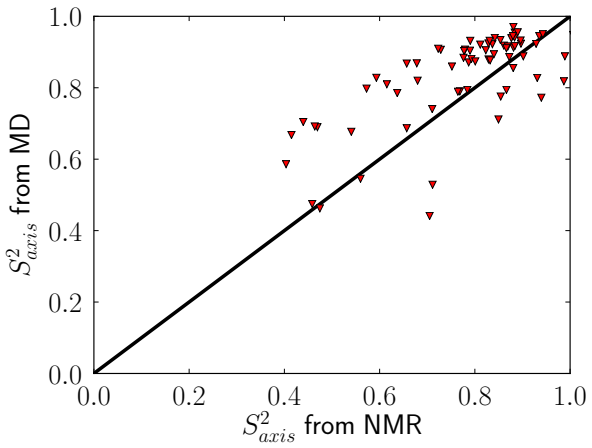

Figure S4: Correlation of methyl order parameters of T4L from NMR relaxation and MD simulations using direct fitting of the Lipari-Szabo TCF with fixed $\tau_{R,i}$'s for the LS2 methyls.

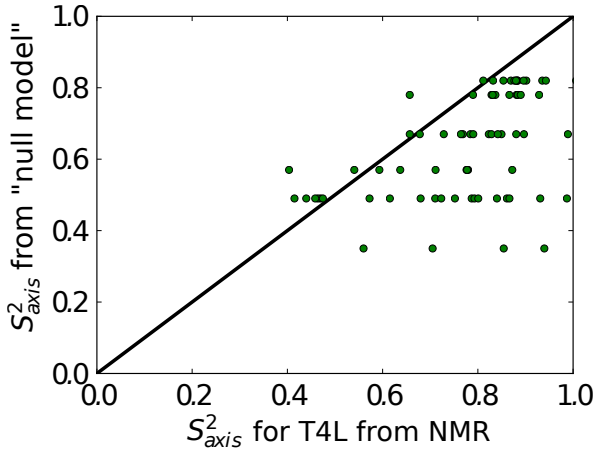

Figure S5: Correlation of methyl order parameters of T4L from NMR relaxation and a null model from NMR relaxation experiments of 12 different proteins with published side-chain dynamics data. The data used for the null model are from ubiquitin,[S6] the third fnIII domain from tenascin,[S7] tenth fnIII domain from fibronectin,[S7] adipocyte lipid binding protein,[S8] muscle fatty acid binding protein,[S8] phospholipase Cγ1 SH2 domain,[S9] oxidized flavodoxin,[S10] HIV protease,[S11] cytochrome c2,[S12] A3D,[S13] Fyn SH3,[S14] mouse urinary protein,[S15] troponin C.[S16] The average S^2_{axis} values are: ALA-C$^\beta$ 0.82, ILE-C$^\delta$ 0.57, ILE-C$^\gamma$ 0.78, LEU-C$^\delta$ 0.49, MET-C$^\epsilon$ 0.35, THR-C$^\gamma$ 0.72, VAL-C$^\gamma$ 0.67.

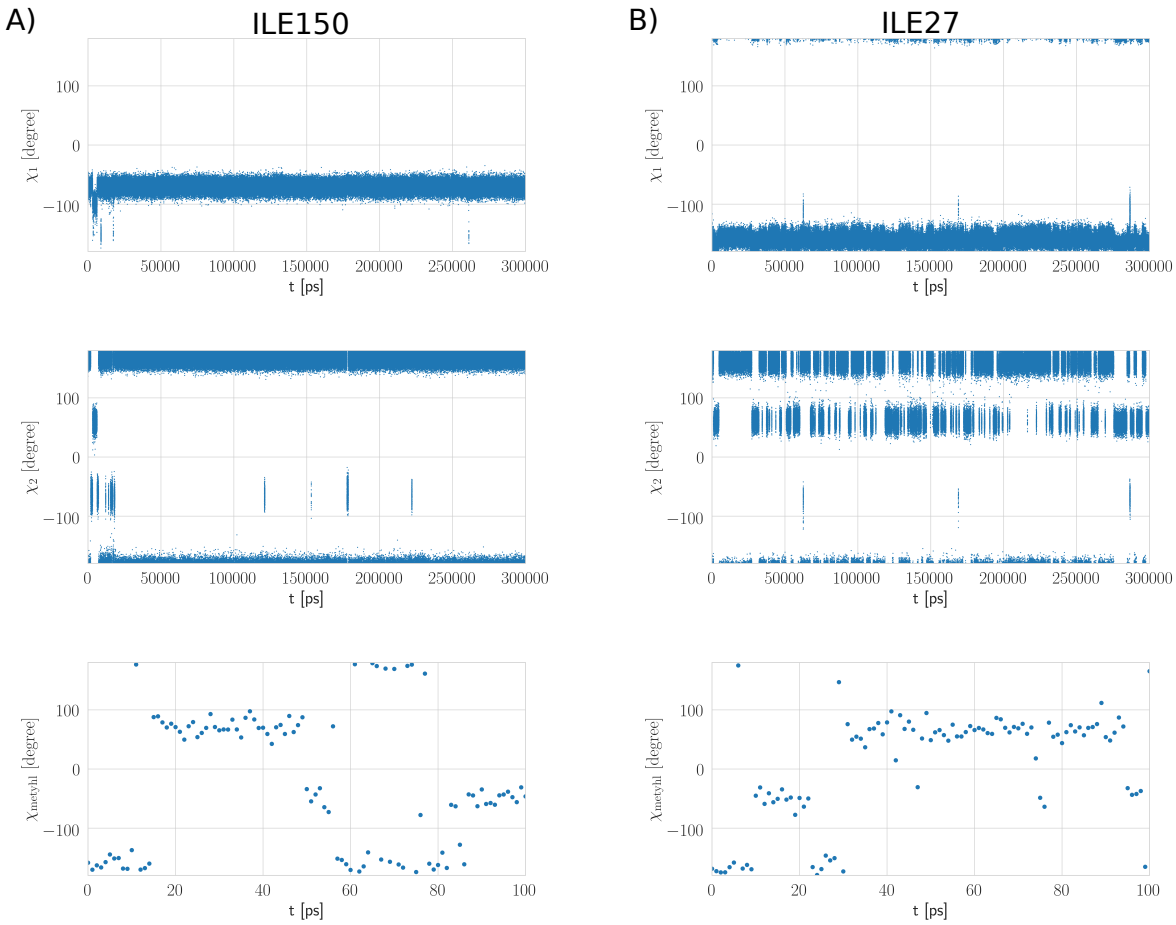

Figure S6: Side-chain dihedral angles χ_1 (top), χ_2 (center), and χ_{methyl} (bottom) of ILE150 (A) and ILE27 (B) from a representative MD simulation. For methyl spinning (χ_{methyl}) only the first 100 ps are shown.

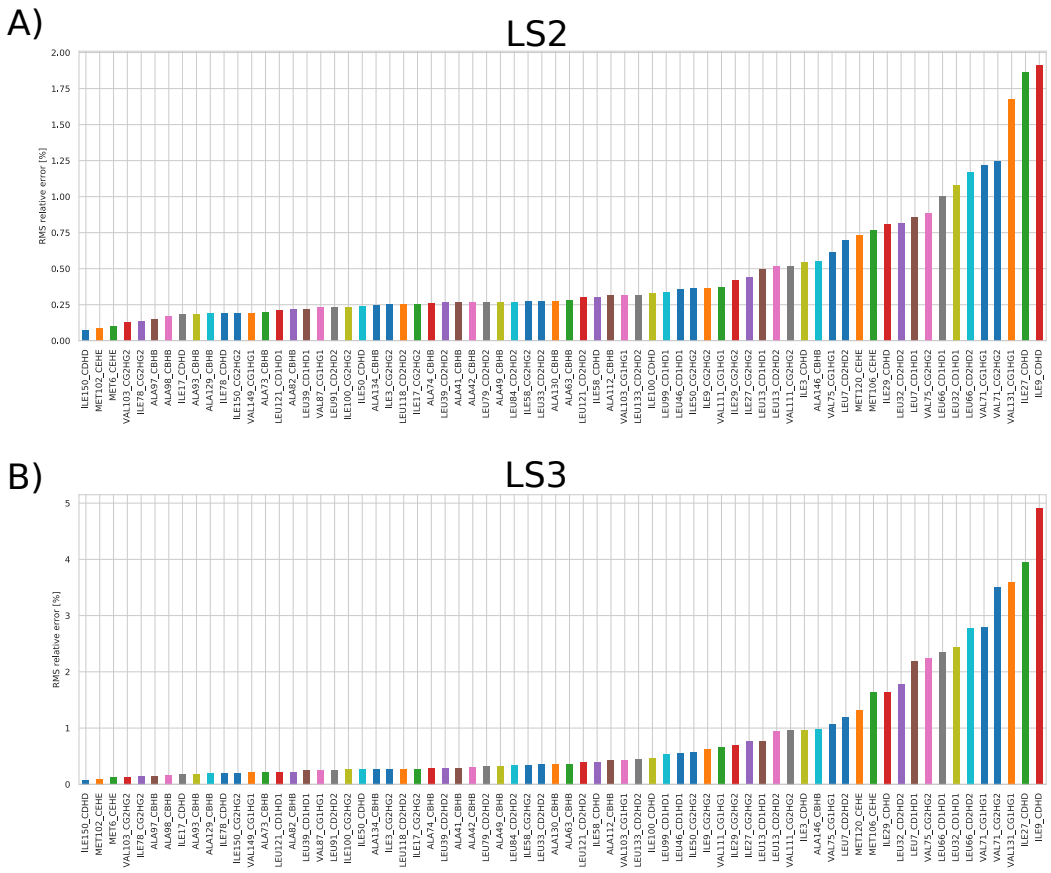

Figure S7: Root mean square relative error of all methyl groups, sorted in increasing order, for LS2 (A) and LS3 (B).

References

(S1) Mulder, F. A. A. *ChemBioChem* **2009**, *10*, 1477–1479.

(S2) Mulder, F. A. A.; Hon, B.; Mittermaier, A.; Dahlquist, F. W.; Kay, L. E. *J. Am. Chem. Soc.* **2002**, *124*, 1443–1451.

(S3) Xue, Y.; Pavlova, M. S.; Ryabov, Y. E.; Reif, B.; Skrynnikov, N. R. *J. Am. Chem. Soc.* **2007**, *129*, 6827–6838.

(S4) Viguera, A. R.; Serrano, L. *J. Mol. Biol.* **2001**, *311*, 357–371.

(S5) Agarwal, V.; Diehl, A.; Skrynnikov, N.; Reif, B. *J. Am. Chem. Soc.* **2006**, *128*, 12620–12621.

(S6) Liao, X.; Long, D.; Li, D.-W.; Brüschweiler, R.; Tugarinov, V. *J. Phys. Chem. B* **2012**, *116*, 606–620.

(S7) Best, R. B.; Rutherford, T. J.; Freund, S. M. V.; Clarke, J. *Biochemistry* **2004**, *43*, 1145–1155.

(S8) Constantine, K. L.; Friedrichs, M. S.; Wittekind, M.; Jamil, H.; Chu, C.-H.; Parker, R. A.; Goldfarb, V.; Mueller, L.; Farmer, B. T. *Biochemistry* **1998**, *37*, 7965–7980.

(S9) Muhandiram, D. R.; Yamazaki, T.; Sykes, B. D.; Kay, L. E. *J. Am. Chem. Soc.* **1995**, *117*, 11536–11544.

(S10) Liu, W.; Flynn, P. F.; Fuentes, E. J.; Kranz, J. K.; McCormick, M.; Wand, A. J. *Biochemistry* **2001**, *40*, 14744–14753.

(S11) Ishima, R.; Petkova, A. P.; Louis, J. M.; Torchia, D. A. *J. Am. Chem. Soc.* **2001**, *123*, 6164–6171.

(S12) Flynn, P. F.; Bieber Urbauer, R. J.; Zhang, H.; Lee, A. L.; Wand, A. J. *Biochemistry* **2001**, *40*, 6559–6569.

(S13) Walsh, S. T. R.; Lee, A. L.; DeGrado, W. F.; Wand, A. J. *Biochemistry* **2001**, *40*, 9560–9569.

(S14) Mittermaier, A.; Davidson, A. R.; Kay, L. E. *J. Am. Chem. Soc.* **2003**, *125*, 9004–9005.

(S15) Chaykovski, M. M.; Bae, L. C.; Cheng, M.-C.; Murray, J. H.; Tortolani, K. E.; Zhang, R.; Seshadri, K.; Findlay, J. H. B. C.; Hsieh, S.-Y.; Kalverda, A. P.; Homans, S. W.; Brown, J. M. *J. Am. Chem. Soc.* **2003**, *125*, 15767–15771.

(S16) Gagné, S. M.; Tsuda, S.; Spyracopoulos, L.; Kay, L. E.; Sykes, B. D. *J. Mol. Biol.* **1998**, *278*, 667–686.